

1 We thank the editor and reviewers for their thoughtful comments. We have responded to each  
2 comment and made appropriate changes to the manuscript. **Reviewer comments are in bold**, author  
3 responses are in plain text. A tracked-changes version of the manuscript and the SI is appended below  
4 our responses.

5 **Editor comments:**

6 **Introduction (p. 5/l. 9) and conclusions (19/12):**

7 **Please add a caveat that previous modelling efforts have made different assumptions about the**  
8 **preferential transfer of central and terminal O atoms to NO<sub>2</sub> and NO<sub>3</sub>, and the <sup>17</sup>O enrichment of**  
9 **different ozone isotopomers. This is still not clear enough.**

10 This has been added to the last paragraph of the Introduction. It now reads:

11 “Previous modeling studies showed good agreement with observations of  $\Delta^{17}\text{O}(\text{nitrate})$  when assuming  
12 that the bulk oxygen isotopic composition of ozone ( $\Delta^{17}\text{O}(\text{O}_3)$ ) is equal to 35‰ (Alexander et al.,  
13 2009;Michalski et al., 2003), but varied in their assumption on terminal oxygen atom versus statistical  
14 isotopic transfer from O<sub>3</sub> to the reactant (NO and NO<sub>2</sub>). This is an important distinction because it is  
15 now known that the <sup>17</sup>O enrichment in O<sub>3</sub> is contained entirely in its terminal oxygen atoms, and it is the  
16 terminal oxygen atom that is transferred from O<sub>3</sub> (Vicars et al., 2012;Berhanu et al., 2012;Bhattacharya  
17 et al., 2008;Savarino et al., 2008;Michalski and Bhattacharya, 2009;Bhattacharya et al., 2014), so that  
18 the  $\Delta^{17}\text{O}$  value of the oxygen atom transferred from ozone to the product is 50% larger than the bulk  
19  $\Delta^{17}\text{O}(\text{O}_3)$  value.”

20 Some of the wording above was previously at the end of the Methods section, and has been removed to  
21 avoid unnecessary repetition.

22

23 **5/2: Remove tilde sign and adjust interval to encompass full range of observations (6 to 54 ‰ based**  
24 **on Krankowsky et al. 1995; 19 to 41 ‰ based on Johnston & Thiemens 1997).**

25

26 Done.

27

28 **5/4: Likewise, the range shown here is too narrow. It's 30 to 46 ‰ for Morton et al. (1990). Please**  
29 **also add "et al." to the reference.**

30 Done.

31

32 **17/26 & 20/1: Replace tilde sign by actual range value with uncertainty. All measurement results**  
33 **should be rounded according to their uncertainty and stated with an estimate of their measurement**  
34 **uncertainty. Approximation symbols should therefore not be used (unless you are approximating a**  
35 **mathematically exact number, e.g.  $\pi \approx 3.14$ ). In any case, the correct approximation symbol has two**  
36 **wavy lines ( $\approx$ ). It is not the tilde sign ( $\sim$ ), a symbol which has perhaps made it into the literature due to**  
37 **limitations of early typewriters.**

38 Thank you for this point. I have included the exact range. As part of this I found a typo, what said  
39 “increases” should have said “decreases”.

1  
2 **Figure S1: More than half of the plot appears with the color corresponding to the colorbar maximum.**  
3 **Please include a variant of the plot with an increased maximum value so that variations in  $\tau \geq 2$  d can**  
4 **be distinguished, or perhaps add contour lines for values higher than 2 days.**

5 I have remade this plot on the log scale and included the full range of calculated values.

6  
7 **Figure S3: Please explain the meaning of the dashed lines in the figure caption.**

8 I have added the following to the Figure 5 and Figure S3 captions:

9 "The  $y=x$  (solid line) and  $y = 2x$  and  $y = 0.5x$  (dashed) are shown."

10

11 **Figure S6: The caption should refer to Fig. S3.**

12 Thanks for catching this. It has been fixed.

13

14 **Anonymous Referee #2:**

15 **The authors have certainly improved the manuscript in response to the reviewer's comments.**  
16 **Submission of the revised manuscript and continuing onto publication in ACP is warranted. There are**  
17 **few areas that the authors should revisit and consider further revision based upon the original**  
18 **reviewers' comments:**

19

20 **(1) The authors added a qualitative explanation for the lack of agreement with observations in Mt.**  
21 **Lulin as lack of heterogeneous chemistry "due to minimal aerosol surface area." However, this**  
22 **statement contrasts with the conclusions drawn in the Guha et al. observational study, so the**  
23 **response by the authors needs to be refined to better explain this interpretation (do they mean that**  
24 **the model predicted aerosol surface area is too lacking to have heterogeneous chemistry?).**

25 Indeed there does seem to be a discrepancy between the interpretation of the observations at Mt. Lulin  
26 in Guha et al. with both subsequent observations in Beijing and in the model. I point out the former by  
27 stating that although the authors of the Mt. Lulin paper state that nitrate is transported to Mt. Lulin  
28 from polluted regions, that this is not consistent with the observations in Beijing, which show much  
29 higher  $\Delta^{17}\text{O}(\text{nitrate})$  values than what was measured at Mt. Lulin. If transport from polluted regions was  
30 the reason for the model-observation discrepancy, one might expect that the model would  
31 underestimate the observations, and the opposite occurs. Thus I'm suggesting that the reason for the  
32 model-observation discrepancy is that this location receives transport from the free troposphere, where  
33  $\text{NO}_2+\text{OH}$  dominates nitrate formation. To make this more clear, I have added the following sentence to  
34 this paragraph:

35 "Low  $\Delta^{17}\text{O}(\text{nitrate})$  values from nitrate formed at higher altitudes and transported to Mt. Lulin would not  
36 be accounted for in the model since the isotopes are not transported."

37

38 **(2) The authors make the excuse in considering a comment about the Wang et al., GCA, 2014 paper**  
39 **and the Fibiger et al., 2016 paper that the data is "not available". It has long been the practice to**

1 contact corresponding authors for data if it is not available in the manuscript. And I found that the  
2 Fibiger et al., 2016 reference actually states the following: Data from this paper are available at  
3 ACADIS. Data sets [https://www.aoncadis.org/project/collaborative\\_research\\_the\\_](https://www.aoncadis.org/project/collaborative_research_the_impact_of_bromine_chemistry_on_the_isotopic_composition_of_nitrate_at_summit_greenland.html)  
4 [impact\\_of\\_bromine\\_chemistry\\_on\\_the\\_isotopic\\_composition\\_of\\_nitrate\\_at\\_](https://www.aoncadis.org/project/collaborative_research_the_impact_of_bromine_chemistry_on_the_isotopic_composition_of_nitrate_at_summit_greenland.html)  
5 [summit\\_greenland.html](https://www.aoncadis.org/project/collaborative_research_the_impact_of_bromine_chemistry_on_the_isotopic_composition_of_nitrate_at_summit_greenland.html).  
6

7 Looking at this website it appears to include the isotope data from both Fibiger et al 2016 and Fibiger  
8 et al 2013 (the 2013 one reports the D17O data). The D17O data from the Fibiger et al., 2013  
9 (Geophysical Research Letters, VOL. 40, 3484–3489, doi:10.1002/grl.50659, 2013) should be  
10 considered in the current study and does include values that look to be close to 39 per mil (or at least  
11 definitely >>30 per mil!). The authors should revisit this and consider the implications for their  
12 response in the manuscript. Also consider contacting F. Wang or G. Michalski for the data from Wang  
13 et al. so this can be included as well.  
14

15 I have contacted the authors of these papers and obtained the data. I have included the data from  
16 Fibiger et al. [2013] in Figures 5 and 6 (and in the related figures in the supplement) and the Wang et al.  
17 [2014] data in Figure 5. I include only the concentration weighted, monthly mean measurements from  
18 Summit in June of 2010 and 2011. Although there were also measurements in May, it was only for the  
19 second half of May. Since May is in the shoulder season, there may be a significant difference between  
20 early and late May, and I have only output monthly means from the model. This adds two data points to  
21 Figures 5 and 6. The error bars in Figure 6 for the Fibiger et al. data reflect the standard deviation of the  
22 measurements, and this is stated in the figure caption. The Wang et al paper adds one data point to  
23 Figure 5. Although there were measurements at 9 different locations, all 9 locations are in the same  
24 model grid box. I calculated the concentration weighted monthly mean from observations at all 9  
25 locations, and compared with the mean  $\Delta^{17}\text{O}(\text{nitrate})$  from the model from July – December, which is  
26 when the measurements occurred. In sum, these data sets add 3 additional data points to Figure 5, and  
27 together do not change the statistics.

28  
29 **(3) The statement added by the authors that “Although lack of transport of the isotope tracers hinders**  
30 **direct comparison of the model with observations at any particular location” contrasts with the fact**  
31 **that they make direct comparison with a range of time series in Figure 5. So maybe restate this that**  
32 **the lack of transport adds uncertainty to direct comparisons – but you do make direct comparisons in**  
33 **space and in time!**

34  
35 Thanks for this suggestion. This has been changed to the following:

36 “Although lack of transport of the isotope tracers adds uncertainty to direct comparison of the model  
37 with observations at any particular location, ...”

38  
39 **(4) The phrasing of “the influence of clouds on nitrate formation” does not really make sense. This**  
40 **should be rephrased to account for the fact that precipitation will represent a column average of**  
41 **nitrate (i.e. long-range transported nitrate, nitrate formed in clouds, and nitrate formed near the**

1 surface). The point that the meteorology tends to have clouds near 1 km means that the model  
2 sampling is robust for comparison on this point, but the impact of clouds on nitrate formation does  
3 not seem to be the point here.

4 I am referring to the influence of clouds on the *chemistry* of nitrate formation here, not on the influence  
5 of wet deposition on nitrate abundance. This is because the model now includes nitrate formation  
6 chemistry in cloud droplets. For clarity, this has been restated as follows:

7 “However, since cloud water peaks on average near 1 km altitude in the MERRA2 meteorology used to  
8 drive GEOS-Chem, our model sampling strategy should capture the majority of the influence of clouds  
9 on the *chemistry* of nitrate formation.”

10

11 **(5) It is not clear whether the authors added a clear reasoning for the cloud chemistry simulation  
12 versus the standard simulation to the manuscript. (Response to comment marked “Page 16, Section  
13 4.2”). The manuscript needs to be clear about how, when and where the results from different  
14 simulations are being used and why.**

15 We state in the paper that we focus on the “cloud chemistry” simulation because we consider it the  
16 state of the science. All other simulations are presented in Section 4, as stated here in the manuscript.  
17 We have added a justification for why we conduct sensitivity simulations relative to the “standard”  
18 model, as shown below:

19 “Additional model sensitivity studies are also performed and examined relative to the “standard” model  
20 simulation, which represents a more common representation of nitrate chemistry in atmospheric  
21 chemistry models.”

22

23 **(6) Regarding the comments on understanding D17O(NO<sub>3</sub><sup>-</sup>) more regionally (e.g., showing how  
24 D17O(NO<sub>3</sub><sup>-</sup>) changes regionally based upon the sensitivity studies). Perhaps another way to consider  
25 this is to add a figure to the SI that shows the results of the different simulations for the times series  
26 comparison with observations (ie Figure 6). This would give much more quantitative information for  
27 researchers conducting observations and give much more information about how sensitive the D17O  
28 is in different regions where these processes are more/most important in different seasons. This  
29 would only add 1 figure to the SI (i.e. Figure 6 with different color lines representing a few different  
30 sensitivity simulations?).**

31 I have replaced Figure S4. The old Figure S4 showed the results from the “standard” simulation. The new  
32 Figure S4 shows results from all of the simulations (total of 7). A figure with different colors for each  
33 simulation was hard to read because of the large number of simulations. Instead I show the “cloud  
34 chemistry” simulation again as points, but with error bars reflecting the full range from all sensitivity  
35 studies. In the main text (Figure 6), the error bars are different, and instead reflect the estimated  
36 impact of assuming isotopic equilibration in Mt. Lulin, which is near populated regions in China where  
37 nighttime nitrate formation is relatively fast.

38

39 **(7) The dashed lines in Figure 5 appear to represent +/- 50%. These should be defined in the figure**

1 **caption and the authors should consider whether it would make more sense to include dashed lines at**  
2 **+/- 25%.**

3 This is now explicit in the captions of Figure 5 and Figure S3.

4

5

6

7 **Greg Michalski:**

8 **The authors have substantially improved their manuscript. However I believe they need more**  
9 **thoroughly and directly address two issues raised by several of the reviewers.**

10

11 **1) The troublesome of value of the O3 D17O value as some fixed value. Using Vicars et al. data does**  
12 **not address the T and P effect demonstrated by numerous lab experiments. The argument that**  
13 **stratospheric O3 "resets" avoids the issue. Any NO oxidation or NO3- production above the mixed**  
14 **layer will likely have a different D17O because the O3 D17O in those layers will be a function of T and**  
15 **P and not fixed at 25 permil. The authors seem to argue that using 25 best "fits the data". This seems**  
16 **a circular argument. One could also argue that the experimental O3 D17O are correct and the**  
17 **pathways are actually wrong. There should be a measure of NO3- production in each model**  
18 **layer...How important is NO3- production at say 5 km and what might the O3 D17O be t this T and P?**  
19 **It would be difficult to hash all this out in the current paper but my fear is that there is a mantra of "its**  
20 **25 permil always and everywhere" is being repeated by a host of recent papers at the expense of**  
21 **numerous other studies that say otherwise. This makes it increasing difficult to challenge. There**  
22 **should be a least one paragraph that there is somethings we don't understand about O3 D17O and a**  
23 **critical assessment of these conflicting estimates.**

24 You are correct that the  $\Delta^{17}\text{O}(\text{O}_3)$  observations from Vicars et al. are at the surface, and thus may not  
25 represent the value of  $\Delta^{17}\text{O}(\text{O}_3)$  in the free troposphere. Fortunately for this model-observation  
26 comparison, the  $\Delta^{17}\text{O}(\text{nitrate})$  observations are also at the surface. I've added some additional  
27 discussion on this topic to the last paragraph of the introduction. The end of this last paragraph now  
28 reads:

29 "Note that laboratory studies show that the magnitude of  $\Delta^{17}\text{O}(\text{O}_3)$  is dependent on temperature and  
30 pressure (Heidenreich and Thiemens, 1986;Thiemens, 1990;Morton et al., 1990). The observations of  
31  $\Delta^{17}\text{O}(\text{O}_3)$  by Vicars et al. (2012, 2013) were at the surface over a large temperature range, but may not  
32 reflect the value of  $\Delta^{17}\text{O}(\text{O}_3)$  at higher altitudes. However, with the exception of lightning, whose  
33 emissions are presently several times smaller than  $\text{NO}_x$  emissions from anthropogenic and biomass  
34 burning sources (Murray, 2016),  $\text{NO}_x$  sources emit at the surface. With a  $\text{NO}_x$  lifetime relative to its  
35 conversion to nitrate on the order of one day (Levy et al., 1999), most nitrate formation also occurs near  
36 the surface. Here, we examine the relative contribution of each nitrate formation pathway in a global  
37 chemical transport model and compare the model with surface observations of  $\Delta^{17}\text{O}(\text{nitrate})$  from  
38 around the world."

39

40 **2) The role of NO emissions at night is still not satisfactory addressed. Morin et al.s model did not**

1 include emissions, thus their conclusions about 5% are not valid. In most of the domain of a global  
2 model the nighttime emissions are comparable to daytime. Only urban areas with vehicles is there a  
3 significant difference between daytime and night emissions. Thus NO emitted at night retains its  
4 source O until sunrise scrambling. How much of this oxidized at night to NO<sub>2</sub> to exchange or form  
5 NO<sub>3</sub>? Clearly this would have a major impact in high latitudes in the winter. Are we to be convinced  
6 the NO emitted in Alaska in Jan. is photochemically equilibrated with O<sub>3</sub> within 5%? Seem  
7 implausible. I do not expect the authors to redo their model, but there should be another full  
8 paragraph is the discussion of the limits of the equilibration assumption.  
9

10 I agree that the results of Morin et al are not valid since they did not emit NO at night. I've deleted the  
11 sentence referencing this paper.

12 To estimate the error due to the assumption of isotopic equilibration of NO<sub>x</sub> in the model, we calculate  
13 the lifetime of NO<sub>x</sub> against oxidation to nitrate from the chemical pathways that only occur at night. This  
14 is plotted in Figure S1 (which has been revised to show the full range of calculated values). The shorter  
15 the NO<sub>x</sub> lifetime against nighttime oxidation, the more likely it is that NO emitted at night will be  
16 oxidized to nitrate before sunrise. Figure S1 shows that the shortest lifetime against nighttime oxidation  
17 is 0.4 days and that lifetimes less than one day occur in only very few locations. Over the majority of the  
18 globe, the lifetime of NO<sub>x</sub> against oxidation at night is > 1 day, suggesting that the majority of NO  
19 emitted at night will survive until sunrise prior to oxidation to nitrate.

20 We investigate the uncertainty in the assumption of NO<sub>x</sub> isotopic equilibration by assuming that half of  
21 total nitrate measured forms at night from NO that was emitted during that same night (i.e., NO<sub>x</sub> is not  
22 isotopically equilibrated during the daytime before being oxidized to nitrate). This effectively assumes  
23 that all nitrate emitted at night is oxidized at night prior to sunrise, which is very likely an overestimate  
24 of the true bias. We make this calculation for Mt. Lulin, because it is in a region (China) with NO<sub>x</sub>  
25 lifetimes against nighttime oxidation that are less than one day. This uncertainty is represented as error  
26 bars for this location in Figure 6, and as you can see cannot account for the model-observation  
27 discrepancy. If this assumption were an issue in the model, one would expect that the model would  
28 overestimate  $\Delta^{17}\text{O}(\text{nitrate})$  in such regions; however, the opposite is the case for Beijing, where the  
29 model underestimates the observations (as shown in Figure 5 and discussed in the text).

30 Certainly if NO<sub>x</sub> is emitted at a high enough latitude that experiences 24-hours of darkness during  
31 winter, there will be no photochemical isotopic equilibration. However, it is also likely that any nitrate  
32 measured at that location will have formed at lower latitudes and transported to higher latitudes, as  
33 NO<sub>x</sub> emissions in polar regions have very low (if any) local NO<sub>x</sub> emissions.

34 For your Alaska example, it will depend on location. Alaska is a big state, and the most northern parts  
35 may experience 24-hours of darkness. Fairbanks, for example, does not fall into this category, as it has  
36 over 3 hours of sunlight on the winter solstice. It would certainly be an interesting case study though.  
37 Since the winter days are short and air pollution can be quite high, one might expect this to be a location  
38 that would experience nighttime oxidation fast enough (long nights with high aerosol surface area) that  
39 a significant fraction of NO is both emitted and oxidized at night prior to sunrise. I know that the  
40 Savarino group is measuring both  $\Delta^{17}\text{O}(\text{NO}_x)$  and  $\Delta^{17}\text{O}(\text{nitrate})$  at this location, and I look forward to  
41 seeing their results as it will be a nice observational constraint on the magnitude of the bias in the  
42 model when assuming photochemical equilibrium.

# 1 Global inorganic nitrate production mechanisms: Comparison 2 of a global model with nitrate isotope observations

Formatted: Indent: Left: 0"

3  
4 Becky Alexander<sup>1</sup>, Tomás Sherwen<sup>2,3</sup>, Christopher D. Holmes<sup>4</sup>, Jenny A. Fisher<sup>5</sup>, Qianjie  
5 Chen<sup>1,6</sup>, Mat J. Evans<sup>2,3</sup>, Prasad Kasibhatla<sup>7</sup>

6  
7 <sup>1</sup>Department of Atmospheric Sciences, University of Washington, Seattle, WA 98195, USA

8 <sup>2</sup>Wolfson Atmospheric Chemistry Laboratories, Department of Chemistry, University of York, York YO10 5DD, UK

9 <sup>3</sup>National Center for Atmospheric Science, University of York, York YO10 5DD, UK

10 <sup>4</sup>Department of Earth, Ocean and Atmospheric Science, Florida State University, Tallahassee, FL 32306, USA

11 <sup>5</sup>Centre for Atmospheric Chemistry, University of Wollongong, Wollongong, New South Wales 2522, Australia

12 <sup>6</sup>Now at Department of Chemistry, University of Michigan, Ann Arbor, MI 48109, USA

13 <sup>7</sup>Nicholas School of the Environment, Duke University, Durham, NC 27708, USA

14  
15 Correspondence to: Becky Alexander ([beckya@uw.edu](mailto:beckya@uw.edu))

16  
17 **Abstract.** The formation of inorganic nitrate is the main sink for nitrogen oxides ( $\text{NO}_x = \text{NO} + \text{NO}_2$ ). Due to the  
18 importance of  $\text{NO}_x$  for the formation of tropospheric oxidants such as the hydroxyl radical (OH) and ozone,  
19 understanding the mechanisms and rates of nitrate formation is paramount for our ability to predict the atmospheric  
20 lifetimes of most reduced trace gases in the atmosphere. The oxygen isotopic composition of nitrate ( $\Delta^{17}\text{O}(\text{nitrate})$ ) is  
21 determined by the relative importance of  $\text{NO}_x$  sinks, and thus can provide an observational constraint for  $\text{NO}_x$   
22 chemistry. Until recently, the ability to utilize  $\Delta^{17}\text{O}(\text{nitrate})$  observations for this purpose was hindered by our lack  
23 of knowledge about the oxygen isotopic composition of ozone ( $\Delta^{17}\text{O}(\text{O}_3)$ ). Recent and spatially widespread  
24 observations of  $\Delta^{17}\text{O}(\text{O}_3)$ , and motivate an updated comparison of modeled and observed  $\Delta^{17}\text{O}(\text{nitrate})$  and a  
25 reassessment of modeled nitrate formation pathways. Model updates based on recent laboratory studies of  
26 heterogeneous reactions renders dinitrogen pentoxide ( $\text{N}_2\text{O}_5$ ) hydrolysis as important as  $\text{NO}_2 + \text{OH}$  (both 41%) for

1 global inorganic nitrate production near the surface (below 1 km altitude). All other nitrate production mechanisms  
2 individually represent less than 6% of global nitrate production near the surface, but can be dominant locally. Updated  
3 reaction rates for aerosol uptake of NO<sub>2</sub> result in significant reduction of nitrate and nitrous acid (HONO) formed  
4 through this pathway in the model, and render NO<sub>2</sub> hydrolysis a negligible pathway for nitrate formation globally.  
5 Although photolysis of aerosol nitrate may have implications for NO<sub>x</sub>, HONO and oxidant abundances, it does not  
6 significantly impact the relative importance of nitrate formation pathways. Modeled Δ<sup>17</sup>O(nitrate) (28.6 ± 4.5‰)  
7 compares well with the average of a global compilation of observations (27.6 ± 5.0‰) when assuming Δ<sup>17</sup>O(O<sub>3</sub>) =  
8 26‰, giving confidence in the model's representation of the relative importance of ozone versus HO<sub>x</sub> (= OH + HO<sub>2</sub>  
9 + RO<sub>2</sub>) in NO<sub>x</sub> cycling and nitrate formation on the global scale.

10

## 11 **1. Introduction**

12

13 Nitrogen oxides (NO<sub>x</sub> = NO + NO<sub>2</sub>) are a critical ingredient for the formation of tropospheric ozone (O<sub>3</sub>).  
14 Tropospheric ozone is a greenhouse gas, is a major precursor for the hydroxyl radical (OH), and is considered an air  
15 pollutant due to its negative impacts on human health. The atmospheric lifetime of NO<sub>x</sub> is determined by its oxidation  
16 to inorganic and organic nitrate. The formation of inorganic nitrate (HNO<sub>3</sub>(g) and particulate NO<sub>3</sub><sup>-</sup>) is the dominant  
17 sink for NO<sub>x</sub> globally, while formation of organic nitrate may be significant in rural and remote continental locations  
18 (Browne and Cohen, 2014). Organic nitrate as a sink for NO<sub>x</sub> may be becoming more important in regions in North  
19 America and Europe where NO<sub>x</sub> emissions have declined (Zare et al., 2018). Uncertainties in the rate of oxidation of  
20 NO<sub>x</sub> to nitrate has been shown to represent a significant source of uncertainty for ozone and OH formation in models  
21 (e.g., Newsome and Evans (2017)), with implications for our understanding of the atmospheric lifetime of species  
22 such as methane, whose main sink is reaction with OH.

23

24 NO<sub>x</sub> is emitted to the atmosphere primarily as NO by fossil fuel and biomass/biofuel burning, soil microbes, and  
25 lightning. Anthropogenic sources from fossil fuel and biofuel burning and from the application of fertilizers to soil  
26 for agriculture currently dominate NO<sub>x</sub> sources to the atmosphere (Jaeglé et al., 2005). After emission, NO is rapidly  
27 oxidized to NO<sub>2</sub> by ozone (O<sub>3</sub>), peroxy (HO<sub>2</sub>) and hydroperoxy radicals (RO<sub>2</sub>), and halogen oxides (e.g., BrO). During  
28 the daytime, NO<sub>2</sub> is rapidly photolyzed to NO + O at wavelengths (λ) < 398 nm. NO<sub>x</sub> cycling between NO and NO<sub>2</sub>

1 proceeds several orders of magnitude faster than oxidation of  $\text{NO}_x$  to nitrate during the daytime (Michalski et al.,  
2 2003).

3  
4 Formation of inorganic nitrate is dominated by oxidation of  $\text{NO}_2$  by OH during the day and by the hydrolysis of  
5 dinitrogen pentoxide ( $\text{N}_2\text{O}_5$ ) at night (Alexander et al., 2009). Recent implementation of reactive halogen chemistry  
6 in models of tropospheric chemistry show that formation of nitrate from the hydrolysis of halogen nitrates ( $\text{XNO}_3$ ,  
7 where X = Br, Cl, or I) is also a sink for  $\text{NO}_x$  with implications for tropospheric ozone, OH, reactive halogens, and  
8 aerosol formation (Schmidt et al., 2016; Sherwen et al., 2016; Saiz-Lopez et al., 2012; Long et al., 2014; Parrella et al.,  
9 2012; von Glasow and Crutzen, 2004; Yang et al., 2005). Other inorganic nitrate formation pathways include  
10 hydrogen-abstraction of hydrocarbons by the nitrate radical ( $\text{NO}_3$ ), heterogeneous reaction of  $\text{N}_2\text{O}_5$  with particulate  
11 chloride ( $\text{Cl}^-$ ), heterogeneous uptake of  $\text{NO}_2$  and  $\text{NO}_3$ , direct oxidation of NO to  $\text{HNO}_3$  by  $\text{HO}_2$ , and hydrolysis of  
12 organic nitrate (Atkinson, 2000). Inorganic nitrate partitions between the gas ( $\text{HNO}_3(\text{g})$ ) and particle ( $\text{NO}_3^-$ ) phases,  
13 with its relative partitioning dependent upon aerosol abundance, aerosol liquid water content, aerosol chemical  
14 composition, and temperature. Inorganic nitrate is lost from the atmosphere through wet or dry deposition to the  
15 Earth's surface with a global lifetime against deposition on the order of 3-4 days (Park et al., 2004).

16  
17 Formation of inorganic nitrate was thought to be a permanent sink for  $\text{NO}_x$  in the troposphere due to the slow  
18 photolysis of nitrate compared to deposition. However, laboratory and field studies have shown that  $\text{NO}_3^-$  adsorbed  
19 on surfaces is photolyzed at rates much higher than  $\text{HNO}_3(\text{g})$  (Ye et al., 2016). For example, the photolysis of  $\text{NO}_3^-$   
20 in snow grains on ice sheets has a profound impact on the oxidizing capacity of the polar atmosphere (Domine and  
21 Shepson, 2002). More recently, observations of  $\text{NO}_x$  and nitrous acid (HONO) provide evidence of photolysis of  
22 aerosol  $\text{NO}_3^-$  in the marine (Reed et al., 2017; Ye et al., 2016) and continental (Ye et al., 2018; Chen et al., 2019)  
23 boundary layer, with implications for ozone and OH (Kasibhatla et al., 2018).

24  
25 Organic nitrates form during reaction of  $\text{NO}_x$  and  $\text{NO}_3$  with biogenic volatile organic compounds (BVOCs) and their  
26 oxidation products (organic peroxy radicals,  $\text{RO}_2$ ) (Browne and Cohen, 2014; Liang et al., 1998). Products of these  
27 reactions include peroxy nitrates ( $\text{RO}_2\text{NO}_2$ ) and alkyl and multifunctional nitrates ( $\text{RONO}_2$ ) (O'Brien et al., 1995).  
28 Peroxy nitrates are thermally unstable and decompose back to  $\text{NO}_x$  on the order of minutes to days at warm

1 temperatures. Decomposition of longer-lived peroxy nitrates such as peroxyacetyl nitrate (PAN) can provide a source  
2 of  $\text{NO}_x$  to remote environments (Singh et al., 1992). The fate of  $\text{RONO}_2$  is uncertain. First-generation  $\text{RONO}_2$  is  
3 oxidized to form second-generation  $\text{RONO}_2$  species with a lifetime of about a week for the first-generation species  
4 with  $\geq 4$  carbon atoms, and up to several weeks for species with fewer carbon atoms (e.g., days to weeks for methyl  
5 nitrate) (Fisher et al., 2018). Subsequent photolysis and oxidation of second-generation  $\text{RONO}_2$  species can lead to  
6 the recycling of  $\text{NO}_x$  (Müller et al., 2014), although recycling efficiencies are highly uncertain (Horowitz et al.,  
7 2007;Paulot et al., 2009).  $\text{RONO}_2$  can also partition to the particle phase ( $\text{pRONO}_2$ ) contributing to organic aerosol  
8 formation (Xu et al., 2015).  $\text{pRONO}_2$  is removed from the atmosphere by deposition to the surface, or through  
9 hydrolysis to form inorganic nitrate and alcohols (Rindelaub et al., 2015;Jacobs et al., 2014).

10  
11 The oxygen isotopic composition ( $\Delta^{17}\text{O} = \delta^{17}\text{O} - 0.52 \times \delta^{18}\text{O}$ ) of nitrate is determined by the relative importance of  
12 oxidants leading to nitrate formation from the oxidation of  $\text{NO}_x$  (Michalski et al., 2003). Observations of the oxygen  
13 isotopic composition of nitrate ( $\Delta^{17}\text{O}(\text{nitrate})$ ) have been used to quantify the relative importance of different nitrate  
14 formation pathways and to assess model representation of the chemistry of nitrate formation in the present day  
15 (Alexander et al., 2009;Michalski et al., 2003;Costa et al., 2011;Ishino et al., 2017a;Morin et al., 2009;Morin et al.,  
16 2008;Savarino et al., 2007;Kunasek et al., 2008;Savarino et al., 2013;McCabe et al., 2007;Morin et al., 2007;Hastings  
17 et al., 2003;Kaiser et al., 2007;Brothers et al., 2008;Ewing et al., 2007) and in the past from nitrate archived in ice  
18 cores (Sofen et al., 2014;Alexander et al., 2004;Geng et al., 2014;Geng et al., 2017). Ozone-influenced reactions in  
19  $\text{NO}_x$  oxidation lead to high  $\Delta^{17}\text{O}(\text{nitrate})$  values while  $\text{HO}_x$ -influenced reactions lead to  $\Delta^{17}\text{O}(\text{nitrate})$  near zero.  
20 Oxidation by  $\text{XO}$  (where  $\text{X} = \text{Br}, \text{Cl}, \text{or I}$ ) leads to  $\Delta^{17}\text{O}(\text{nitrate})$  values similar to reactions with ozone because the  
21 oxygen atom in  $\text{XO}$  is derived from the reaction  $\text{X} + \text{O}_3$ . Therefore,  $\Delta^{17}\text{O}(\text{nitrate})$  is determined by the relative  
22 importance of  $\text{O}_3 + \text{XO}$  versus  $\text{HO}_x (= \text{OH} + \text{HO}_2 + \text{RO}_2)$  in both  $\text{NO}_x$  cycling and oxidation to nitrate. Although  
23 freshly emitted  $\text{NO}$  will have  $\Delta^{17}\text{O}(\text{NO}) = 0\%$ ,  $\text{NO}_x$  achieves isotopic equilibrium during the daytime due to rapid  
24  $\text{NO}_x$  cycling, so that its  $\Delta^{17}\text{O}$  value ( $\Delta^{17}\text{O}(\text{NO}_x)$ ) is solely determined by the relative abundance of  $(\text{O}_3 + \text{XO})$  to  $(\text{HO}_2$   
25  $+ \text{RO}_2)$  (Michalski et al., 2003).

26  
27 The  $\Delta^{17}\text{O}$  value of  $\text{HO}_x$  ( $\Delta^{17}\text{O}(\text{HO}_x)$ ) is near zero due to isotopic exchange of  $\text{OH}$  with water vapor (Dubey et al.,  
28 1997). Previously, observations of the  $\Delta^{17}\text{O}$  value of ozone ( $\Delta^{17}\text{O}(\text{O}_3)$ ) showed a large range (~~6–20~~ – 5440‰)

1 (Johnston and Thiemens, 1997; Krankowsky et al., 1995), in contrast to laboratory and modeling studies suggesting  
2 that the range of  $\Delta^{17}\text{O}(\text{O}_3)$  in the troposphere should be relatively narrow ( $32 \pm 230-46$  ‰) (Morton et al.,  
3 1990; Thiemens, 1990). The large range of observed  $\Delta^{17}\text{O}(\text{O}_3)$  values is thought to be due to sampling artifacts  
4 (Brenninkmeijer et al., 2003). Uncertainty in the value of  $\Delta^{17}\text{O}(\text{O}_3)$  has been the largest source of uncertainty in  
5 quantification of nitrate formation pathways using observations of  $\Delta^{17}\text{O}(\text{nitrate})$  (Alexander et al., 2009). Previous  
6 modeling studies showed good agreement with observations of  $\Delta^{17}\text{O}(\text{nitrate})$  when assuming that the bulk oxygen  
7 isotopic composition of ozone ( $\Delta^{17}\text{O}(\text{O}_3)$ ) is equal to 35% (Alexander et al., 2009; Michalski et al., 2003); but varied  
8 in their assumption on terminal oxygen atom versus statistical isotopic transfer from  $\text{O}_3$  to the reactant ( $\text{NO}$  and  $\text{NO}_2$ ).  
9 This is an important distinction because it is now known that the  $^{17}\text{O}$  enrichment in  $\text{O}_3$  is contained entirely in its  
10 terminal oxygen atoms, and it is the terminal oxygen atom that is transferred from  $\text{O}_3$  (Vicars et al., 2012; Berhanu et  
11 al., 2012; Bhattacharya et al., 2008; Savarino et al., 2008; Michalski and Bhattacharya, 2009; Bhattacharya et al., 2014).  
12 so that the  $\Delta^{17}\text{O}$  value of the oxygen atom transferred from ozone to the product is 50% larger than the bulk  $\Delta^{17}\text{O}(\text{O}_3)$   
13 value. Recently, much more extensive observations of  $\Delta^{17}\text{O}(\text{O}_3)$  using a new technique (Vicars et al., 2012)  
14 consistently show  $\Delta^{17}\text{O}(\text{O}_3) = 26 \pm 1\%$  in diverse locations (Vicars et al., 2012; Ishino et al., 2017b; Vicars and  
15 Savarino, 2014), and suggest that previous modeling studies are biased low in  $\Delta^{17}\text{O}(\text{nitrate})$  (e.g., Alexander et al.  
16 (2009)), which would occur if the model underestimated the relative role of ozone in  $\text{NO}_x$  chemistry. These new  
17 observations of  $\Delta^{17}\text{O}(\text{O}_3)$ , combined with improved understanding and hence more comprehensive chemical  
18 representation of nitrate formation in models, motivates an updated comparison of observed and modeled  $\Delta^{17}\text{O}(\text{nitrate})$   
19 as an observational constraint for the relative importance of nitrate formation pathways in the atmosphere. Note that  
20 laboratory studies show that the magnitude of  $\Delta^{17}\text{O}(\text{O}_3)$  is dependent on temperature and pressure (Heidenreich and  
21 Thiemens, 1986; Thiemens, 1990; Morton et al., 1990). The observations of  $\Delta^{17}\text{O}(\text{O}_3)$  by Vicars et al. (2012, 2013)  
22 were at the surface over a large temperature range, but may not reflect the value of  $\Delta^{17}\text{O}(\text{O}_3)$  at higher altitudes.  
23 However, with the exception of lightning, whose emissions are presently several times smaller than  $\text{NO}_x$  emissions  
24 from anthropogenic and biomass burning sources (Murray, 2016).  $\text{NO}_x$  sources emit at the surface. With a  $\text{NO}_x$   
25 lifetime relative to its conversion to nitrate on the order of one day (Levy et al., 1999), most nitrate formation also  
26 occurs near the surface. Here, we examine the relative contribution of each nitrate formation pathway in a global  
27 chemical transport model and compare the model with surface observations of  $\Delta^{17}\text{O}(\text{nitrate})$  from around the world.

Formatted: Subscript

Formatted: Subscript

Formatted: Superscript

Formatted: Subscript

Formatted: Subscript

Formatted: Subscript

Formatted: Subscript

Formatted: Subscript

1  
2  
3  
4  
5  
6  
7  
8  
9  
10  
11  
12  
13  
14  
15  
16  
17  
18  
19  
20  
21  
22  
23  
24  
25  
26  
27  
28

## 2. Methods

We use the GEOS-Chem global chemical transport model version 12.0.0 driven by assimilated meteorology from the MERRA-2 reanalysis product with a native resolution of  $0.5^\circ \times 0.625^\circ$  and 72 vertical levels from the surface up to the 0.01 hPa pressure level. For computational expediency, the horizontal and vertical resolution were downgraded to  $4^\circ \times 5^\circ$  and 47 vertical levels. GEOS-Chem was originally described in Bey et al. (2001) and includes coupled  $\text{HO}_x$ - $\text{NO}_x$ -VOC-ozone-halogen-aerosol tropospheric chemistry as described in Sherwen et al. (2016) and Sherwen et al. (2017) and organic nitrate chemistry as described in Fisher et al. (2016). Aerosols interact with gas-phase chemistry through the effect of aerosol extinction on photolysis rates (Martin et al., 2003) and heterogeneous chemistry (Jacob, 2000). The model calculates deposition for both gas species and aerosols (Liu et al., 2001; Zhang et al., 2001; Wang et al., 1998).

Global anthropogenic emissions, including  $\text{NO}_x$ , are from the Community Emissions Data System (CEDS) inventory from 1950 – 2014 C.E. (Hoesly et al., 2018a). The CEDS global emissions inventory is overwritten by regional anthropogenic emissions inventories in the U.S. (EPA/NE11), Canada (CAC), Europe (EMEP), and Asia (MIX (Li et al., 2017)). Global shipping emissions are from the International Comprehensive Ocean-Atmosphere Data Set (ICOADS), which was implemented into GEOS-Chem as described in Lee et al. (2011).  $\text{NO}_x$  emissions from ships are processed using the PARANOX module described in Vinken et al. (2011) and Holmes et al. (2014) to account for non-linear, in-plume ozone and  $\text{HNO}_3$  production. Lightning  $\text{NO}_x$  emissions match the OTD/LIS satellite climatological observations of lightning flashes as described by Murray et al. (2012). Emissions from open fires are from the Global Fire Emissions Database (GFED4.1). Biogenic soil  $\text{NO}_x$  emissions are described in Hudman et al. (2012). Aircraft emissions are from the Aviation Emissions Inventory Code (AEIC) (Stettler et al., 2011).

Chemical processes leading to nitrate formation in GEOS-Chem have expanded since the previous work of Alexander et al. (2009). Figure 1 summarizes the formation of inorganic nitrate in the current model. In the model, NO is oxidized by  $\text{O}_3$ ,  $\text{HO}_2$ ,  $\text{RO}_2$  and halogen oxides ( $\text{XO} = \text{BrO}$ ,  $\text{ClO}$ ,  $\text{IO}$ , and  $\text{OIO}$ ) to form  $\text{NO}_2$ . The reaction of  $\text{NO} + \text{HO}_2$  can also form  $\text{HNO}_3$  directly, although the branching ratio for this pathway is  $< 1\%$  (Butkovskaya et al., 2005).

1 NO<sub>2</sub> can form HNO<sub>3</sub> directly from its reaction with OH and through hydrolysis on aerosol surfaces. NO<sub>2</sub> can react  
2 with XO to form halogen nitrates (BrNO<sub>3</sub>, ClNO<sub>3</sub>, and INO<sub>3</sub>), which can then form HNO<sub>3</sub> upon hydrolysis (as  
3 described in Sherwen et al. (2016)). NO<sub>2</sub> can also react with O<sub>3</sub> to form NO<sub>3</sub>, which can then react with NO<sub>2</sub>,  
4 hydrocarbons (HC), and the biogenic VOCs monoterpenes (MTN) and isoprene (ISOP). Reaction of NO<sub>3</sub> with NO<sub>2</sub>  
5 forms N<sub>2</sub>O<sub>5</sub>, which can subsequently hydrolyze or react with Cl<sup>-</sup> in aerosol to form HNO<sub>3</sub>. Reaction of NO<sub>3</sub> with HC  
6 forms HNO<sub>3</sub> via hydrogen abstraction. Reactions of NO<sub>3</sub> are only important at night due to its short lifetime against  
7 photolysis. Formation of organic nitrate (RONO<sub>2</sub>) was recently updated in the model as described in Fisher et al.  
8 (2016). Reaction of NO<sub>3</sub> with MTN and ISOP can form RONO<sub>2</sub>. RONO<sub>2</sub> also forms from the reaction of NO with  
9 RO<sub>2</sub> derived from OH oxidation of BVOCs. RONO<sub>2</sub> hydrolyzes to form HNO<sub>3</sub> on a timescale of 1 hour. Inorganic  
10 nitrate partitions between the gas (HNO<sub>3</sub>(g)) and particle (NO<sub>3</sub><sup>-</sup>) phase according to local thermodynamic equilibrium  
11 as calculated in the ISORROPIA-II aerosol thermodynamic module (Fountoukis and Nenes, 2007). HNO<sub>3</sub>(g) and  
12 NO<sub>3</sub><sup>-</sup> are mainly lost from the atmosphere via wet and dry deposition to the surface.

13  
14 In the “standard” model, hydrolysis of N<sub>2</sub>O<sub>5</sub>, NO<sub>3</sub> ( $\gamma_{\text{NO}_3} = 1 \times 10^{-3}$ ), and NO<sub>2</sub> ( $\gamma_{\text{NO}_2} = 1 \times 10^{-4}$ ) occur on aerosol surfaces  
15 only. Uptake and hydrolysis of N<sub>2</sub>O<sub>5</sub> on aerosol surfaces depends on the chemical composition of aerosols,  
16 temperature, and humidity as described in Evans and Jacob (2005). Recently, Holmes et al. (2019) updated the  
17 reaction probabilities of the NO<sub>2</sub> and NO<sub>3</sub> heterogeneous reactions in the model to depend on aerosol chemical  
18 composition and relative humidity. Holmes et al. (2019) also updated the N<sub>2</sub>O<sub>5</sub> reaction probability to additionally  
19 depend on the H<sub>2</sub>O and NO<sub>3</sub><sup>-</sup> concentrations in aerosol (Bertram and Thornton, 2009). In addition to these updates  
20 for hydrolysis on aerosol, Holmes et al. (2019) included the uptake and hydrolysis of N<sub>2</sub>O<sub>5</sub>, NO<sub>2</sub>, and NO<sub>3</sub> in cloud  
21 water and ice limited by cloud entrainment rates. We incorporate these updates from Holmes et al. (2019) into the  
22 “cloud chemistry” model to examine the impacts on global nitrate production mechanisms. We consider the “cloud  
23 chemistry” model as state-of-the science, and as such we focus on the results of this particular simulation. Additional  
24 model sensitivity studies are also performed and examined relative to the “standard” model simulation, which  
25 represents a more common representation of nitrate chemistry in atmospheric chemistry models. These additional  
26 sensitivity simulations are described in Section 4.

27

1  $\Delta^{17}\text{O}(\text{nitrate})$  is calculated in the model using monthly-mean, local chemical production rates, rather than by treating  
 2 different isotopic combinations of nitrate as separate tracers that can be transported in the model. Alexander et al.  
 3 (2009) transported four nitrate tracers, one each for nitrate production by  $\text{NO}_2+\text{OH}$ ,  $\text{N}_2\text{O}_5$  hydrolysis,  $\text{NO}_3+\text{HC}$ , and  
 4 nitrate originating from its formation in the stratosphere. Since  $\Delta^{17}\text{O}(\text{NO}_x)$  was not transported in the Alexander et al.  
 5 (2009) model, it was calculated using local production rates, so effectively only one-third of the  $\Delta^{17}\text{O}(\text{nitrate})$  was  
 6 transported in Alexander et al. (2009). Accurately accounting for transport of  $\Delta^{17}\text{O}(\text{nitrate})$  in the model would require  
 7 transporting all individual isotopic combinations of the primary reactant (NO), the final product (nitrate), and each  
 8 reaction intermediate (e.g.,  $\text{N}_2\text{O}_5$ ), which we do not do here due to the large computational costs. Thus, the model  
 9 results shown here represent  $\Delta^{17}\text{O}(\text{nitrate})$  from local  $\text{NO}_x$  cycling and nitrate production. This may lead to model  
 10 biases, particularly in remote regions such as polar-regions in winter-time when most nitrate is likely transported from  
 11 lower latitudes or the stratosphere. This should make less difference in polluted regions where most nitrate is formed  
 12 locally, or for example in polar regions in summer when photochemical recycling of nitrate in the snowpack represents  
 13 a significant local source of  $\text{NO}_x$  at the surface (Domine and Shepson, 2002). Although lack of transport of the isotope  
 14 tracers ~~hinders-adds uncertainty to~~ direct comparison of the model with observations at any particular location, this  
 15 approach will reflect the full range of possible modeled  $\Delta^{17}\text{O}(\text{nitrate})$  values for the current chemical mechanism,  
 16 which can then be compared to the range of observed  $\Delta^{17}\text{O}(\text{nitrate})$  values around the globe.

17  
 18 The  $\Delta^{17}\text{O}(\text{nitrate})$  value of nitrate produced from each production pathway is calculated as shown in Table 1. The  
 19 value of  $A$  in Table 1 represents the relative importance of the oxidation pathways of NO to  $\text{NO}_2$  where the oxygen  
 20 atom transferred comes from ozone ( $\text{NO} + \text{O}_3$  and  $\text{NO} + \text{XO}$ ):

$$21 \quad A = \frac{k_{\text{O}_3+\text{NO}}[\text{O}_3]+k_{\text{XO}+\text{NO}}[\text{XO}]}{k_{\text{O}_3+\text{NO}}[\text{O}_3]+k_{\text{XO}+\text{NO}}[\text{XO}]+k_{\text{HO}_2+\text{NO}}[\text{HO}_2]+k_{\text{RO}_2+\text{NO}}[\text{RO}_2]} \quad (\text{E1})$$

22 In E1,  $k$  represents the local reaction rate constant for each of the four reactions,  $\text{XO} = \text{BrO}$ ,  $\text{ClO}$ ,  $\text{IO}$ , and  $\text{OIO}$ , and  
 23 we assume  $\Delta^{17}\text{O}(\text{XO})$  is equal to the  $\Delta^{17}\text{O}$  value of the terminal oxygen atoms of ozone, as described in more detail  
 24 below. This effectively assumes that the other oxidation pathways ( $\text{NO} + \text{HO}_2$  and  $\text{NO} + \text{RO}_2$ ) yield  $\Delta^{17}\text{O}(\text{NO}_x) =$   
 25  $0\text{‰}$ . Although  $\text{HO}_2$  may have a small  $^{17}\text{O}$  enrichment on the order of 1-2‰ (Savarino and Thiemens, 1999b), the  
 26 assumption that this pathway yields  $\Delta^{17}\text{O}(\text{NO}_x) = 0\text{‰}$  simplifies the calculation and leads to negligible differences in  
 27 calculated  $\Delta^{17}\text{O}(\text{nitrate})$  (Michalski et al., 2003). This approach assumes that  $\text{NO}_x$  cycling is in photochemical steady-

1 state, which only occurs during the daytime.  $A$  is calculated in the model as the 24-hour average  $\text{NO}_2$  production rate,  
2 rather than the daytime average only. As was shown in Alexander et al. (2009), rapid daytime  $\text{NO}_x$  cycling dominates  
3 the calculated 24-hour averaged  $A$  value, leading to negligible differences in calculated  $\Delta^{17}\text{O}(\text{nitrate})$  for 24-hour  
4 averaged values versus daytime averaged values.

5  
6  $\text{NO}_x$  formed during the day will retain its daytime  $\Delta^{17}\text{O}(\text{NO}_x)$  signature throughout the night due to lack of  $\text{NO}_2$   
7 photolysis (Morin et al., 2011), suggesting similar  $A$  values for the nighttime reactions (R2, R4, R5, R8, and R10 in  
8 Table 1). However,  $\text{NO}$  emitted at night will not undergo photochemical recycling; initially suggesting that  $\text{NO}$  will  
9 retain its emitted  $\Delta^{17}\text{O}(\text{NO})$  value of 0‰ prior to sunrise. Thus, any  $\text{NO}$  emitted at night and oxidized to  $\text{NO}_2$  before  
10 sunrise will result in  $\Delta^{17}\text{O}(\text{NO}_2)$  equal to one-half of the  $\Delta^{17}\text{O}$  value of the oxidant, since only one of the two oxygen  
11 atoms of  $\text{NO}_2$  will originate from the oxidant. Since  $\text{HO}_x$  abundance is low at night, ozone will be the dominant  
12 oxidant. Thus,  $\text{NO}$  both emitted and oxidized to  $\text{NO}_2$  at night will lead to  $A_{\text{night}} = 0.5$  (half of the O atoms of  $\text{NO}_2$   
13 originate from  $\text{O}_3$ ). Although isotopic exchange between  $\text{NO} + \text{NO}_2$  (Sharma et al., 1970) and  $\text{NO}_2$  and  $\text{NO}_3$  via  
14 thermal dissociation of  $\text{N}_2\text{O}_5$  (Connell and Johnston, 1979) will tend to increase  $\Delta^{17}\text{O}(\text{NO})$  above its emitted value of  
15 0‰, the bulk  $\Delta^{17}\text{O}$  value of  $\text{NO}_x$  plus  $\text{NO}_3$  system will be lower at night than during the daytime due to the absence  
16 of photochemical cycling at night (Michalski et al., 2014; Morin et al., 2011). Since the atmospheric lifetime of  $\text{NO}_x$   
17 near the surface against nighttime oxidation to nitrate (R2+R4+R5) is typically greater than 24 hours (Figure S1),  
18 most nitrate formed during the nighttime will form from  $\text{NO}_x$  that reached photochemical equilibrium during the  
19 previous day. Thus, we use values of  $A$  calculated as the 24-hour average  $\text{NO}_2$  production rate for calculating the  
20  $\Delta^{17}\text{O}(\text{nitrate})$  value of all nitrate production pathways, including those that can occur at night. ~~This is consistent with~~  
21 ~~a box modeling study that explicitly calculated the diurnal variability of  $\Delta^{17}\text{O}(\text{NO}_x)$  and  $\Delta^{17}\text{O}(\text{nitrate})$  suggesting~~  
22 ~~similar (within 5%) values for  $\Delta^{17}\text{O}(\text{nitrate})$  when assuming the  $\text{NO}_x$  reached photochemical steady state versus~~  
23 ~~explicit calculation of diurnal variability of  $\Delta^{17}\text{O}(\text{NO}_x)$  and  $\Delta^{17}\text{O}(\text{nitrate})$  (Morin et al., 2011).~~ Using 24-hour  
24 averaged  $A$  values may lead to an overestimate of  $\Delta^{17}\text{O}(\text{nitrate})$  in locations with more rapid nighttime nitrate  
25 formation rates such as in China and India (Figure S1). However, even in these locations the lifetime of  $\text{NO}_x$  against  
26 nighttime oxidation is greater than 12 hours, suggesting that over half of nitrate formation at night occurs from the  
27 oxidation of  $\text{NO}_x$  that reached photochemical equilibrium during the daytime. When comparing modeled  $\Delta^{17}\text{O}(\text{nitrate})$

1 with observations, we add error bars to model values in these locations (Beijing and Mt. Lulin, Taiwan) that reflect  
2 the range of possible  $A$  values for nighttime nitrate formation, with the high end ( $A_{high}$ ) reflecting 24-hour average  $A$   
3 values and the low end assuming that half of nitrate formation occurs from oxidation of  $\text{NO}_x$  that reached  
4 photochemical equilibrium during the daytime ( $A_{low} = 0.5A + 0.5A_{night}$ , where  $A_{night} = 0.5$ ).

5  
6  $\Delta^{17}\text{O}(\text{nitrate})$  for total nitrate is calculated in the model according to:

$$7 \quad \Delta^{17}\text{O}(\text{nitrate}) = \sum_{R=R1}^{R10} f_R \Delta^{17}\text{O}(\text{nitrate})_R \quad (\text{E2})$$

8 where  $f_R$  represents the fractional importance of each nitrate production pathway (R1-R10 in Table 1) relative to total  
9 nitrate production, and  $\Delta^{17}\text{O}(\text{nitrate})_R$  is the  $\Delta^{17}\text{O}(\text{nitrate})$  value for each reaction as described in Table 1. To calculate  
10  $\Delta^{17}\text{O}(\text{nitrate})$ , we assume that the mean  $\Delta^{17}\text{O}$  value of the ozone molecule ( $\Delta^{17}\text{O}(\text{O}_3)$ ) is equal to 26‰ based on recent  
11 observations (Vicars et al., 2012; Ishino et al., 2017b; Vicars and Savarino, 2014). ~~Since the  $^{17}\text{O}$  enrichment in  $\text{O}_3$  is~~  
12 ~~contained entirely in its terminal oxygen atoms (Vicars et al., 2012; Berhanu et al., 2012; Bhattacharya et al.,~~  
13 ~~2008; Savarino et al., 2008; Michalski and Bhattacharya, 2009; Bhattacharya et al., 2014), and that it is the terminal~~  
14 ~~oxygen atom that is~~ are transferred to the oxidation product during chemical reactions (Savarino et al., 2008; Berhanu  
15 et al., 2012), ~~the  $\Delta^{17}\text{O}$  value of the oxygen atom transferred from ozone to the product is 50% larger than the bulk~~  
16  ~~$\Delta^{17}\text{O}(\text{O}_3)$  value.~~ Thus, we assume that the  $\Delta^{17}\text{O}$  value of the oxygen atom transferred from  $\text{O}_3$  ( $\Delta^{17}\text{O}(\text{O}_3^*)$ ) = 1.5 x  
17  $\Delta^{17}\text{O}(\text{O}_3)$ , as in previous work (e.g., (Morin et al., 2011)), where  $\Delta^{17}\text{O}(\text{O}_3^*)$  represents the  $\Delta^{17}\text{O}$  value of the terminal  
18 oxygen atoms in ozone. Assuming that  $\Delta^{17}\text{O}(\text{O}_3) = 26\text{‰}$  based on recent observations, this leads to  $\Delta^{17}\text{O}(\text{O}_3^*) = 39\text{‰}$ .

19

20

### 21 3. Results and Discussion

22

23 Figure 1 shows the relative importance of the different oxidation pathways of  $\text{NO}$  to  $\text{NO}_2$  and nitrate formation below  
24 1 km altitude in the model for the “cloud chemistry” simulation, with equivalent values for the “standard” simulation  
25 shown in parentheses. We focus on model results near the surface (below 1 km) because these can be compared to  
26 observations; currently only surface observations of  $\Delta^{17}\text{O}(\text{nitrate})$  are available. We note that two observation data  
27 sets (from Bermuda (Hastings et al., 2003) and Princeton, NJ (Kaiser et al., 2007)) are rainwater samples and thus

1 may represent nitrate formed aloft. However, since cloud water peaks on average near 1 km altitude in the MERRA2  
2 meteorology used to drive GEOS-Chem, our model sampling strategy should capture the majority of the influence of  
3 clouds on [the chemistry of](#) nitrate formation. The dominant oxidant of NO to NO<sub>2</sub> is O<sub>3</sub> (84-85%). Much of the  
4 remaining oxidation occurs due to the reaction with peroxy radicals (HO<sub>2</sub> and RO<sub>2</sub>). Oxidation of NO to NO<sub>2</sub> by XO  
5 is minor (1%) and occurs over the oceans because the main source of tropospheric reactive halogens is from sea salt  
6 aerosol and sea water (Chen et al., 2017; Sherwen et al., 2016; Wang et al., 2018) (Figure 2). In the model, the global,  
7 annual mean lifetime of NO<sub>x</sub> in the troposphere against oxidation to nitrate is about 1 day; about 50% of this loss is  
8 from the reaction of NO<sub>2</sub> + OH. NO<sub>x</sub> loss from N<sub>2</sub>O<sub>5</sub> becomes more important near the surface where aerosol surface  
9 area is relatively high. The global, annual mean lifetime of nitrate in the troposphere against wet and dry deposition  
10 to the surface is about 3 days.

11  
12 For both the “cloud chemistry” and “standard” simulations, the two most important nitrate formation pathways are  
13 NO<sub>2</sub> + OH (41-42%) and N<sub>2</sub>O<sub>5</sub> hydrolysis (28-41%), the latter of which is dominant over the mid- to high-northern  
14 continental latitudes during winter where both NO<sub>x</sub> emissions and aerosol abundances are relatively large (Figures 1  
15 and 3). The “cloud chemistry” simulation results in an equal importance of nitrate formation via NO<sub>2</sub> + OH and N<sub>2</sub>O<sub>5</sub>  
16 hydrolysis (both 41%) due to increases in the rate of N<sub>2</sub>O<sub>5</sub> uptake in clouds and decreases in the importance of NO<sub>2</sub>  
17 hydrolysis, which can compete with N<sub>2</sub>O<sub>5</sub> formation at night. In the “standard” model, NO<sub>2</sub> hydrolysis represents an  
18 important nitrate production mechanism (12%), but it is negligible in the “cloud chemistry” simulation due to the  
19 reduction in the reaction probability (from  $\gamma_{\text{NO}_2} = 10^{-4}$  to  $\gamma_{\text{NO}_2} = 10^{-4}$  to  $10^{-8}$ ) in the model, which is supported by  
20 laboratory studies (Burkholder et al., 2015; Crowley et al., 2010; Tan et al., 2016). The formation of HNO<sub>3</sub> from the  
21 hydrolysis of RONO<sub>2</sub> formed from both daytime (NO + RO<sub>2</sub>) and nighttime (NO<sub>3</sub> + MTN/ISOP) reactions represents  
22 6% of total, global nitrate formation (Figure 1) and is dominant over Amazonia (Figure 3). RONO<sub>2</sub> hydrolysis  
23 represents up to 20% of inorganic nitrate formation in the southeast U.S. (Figure 3). This is similar to Fisher et al.  
24 (2016) who estimated that formation of RONO<sub>2</sub> accounts for up to 20% of NO<sub>x</sub> loss in this region during summer,  
25 with RONO<sub>2</sub> hydrolysis representing 60% of RONO<sub>2</sub> loss. Globally, the formation of inorganic nitrate from the  
26 hydrolysis of RONO<sub>2</sub> is dominated by RONO<sub>2</sub> formation from the daytime reactions (3-6%), while the formation of  
27 RONO<sub>2</sub> from nighttime reactions represents up to 3%. The relative importance of nighttime and daytime RONO<sub>2</sub>

1 formation is expressed as a range because precursors to RONO<sub>2</sub> that formed from monoterpenes can form from both  
2 daytime and nighttime reactions, and these precursors are not separately diagnosed in the model output. HNO<sub>3</sub>  
3 formation from NO<sub>3</sub> + HC and the hydrolysis of XNO<sub>3</sub> are small globally (5-6%). Although XNO<sub>3</sub> hydrolysis is the  
4 dominant nitrate formation pathway over the remote oceans (Figure 3), its contribution to total, global nitrate  
5 production is relatively small due to small local NO<sub>x</sub> sources in these regions.

6  
7 Figures 4 - 6 show modeled  $\Delta^{17}\text{O}(\text{nitrate})$  for the “cloud chemistry” simulation (the “standard” simulation is shown in  
8 Figures S2 – S4). Figure 4 shows modeled annual-mean  $\Delta^{17}\text{O}(\text{nitrate})$  below 1 km altitude ( $\Delta^{17}\text{O}(\text{NO}_2)$  is shown in  
9 Figure S5). The model predicts an annual-mean range of  $\Delta^{17}\text{O}(\text{nitrate}) = 4 - 33\text{‰}$  near the surface. The lowest values  
10 are over Amazonia due to the dominance of RONO<sub>2</sub> hydrolysis and the highest values are over the mid-latitude oceans  
11 due to the dominance of XNO<sub>3</sub> hydrolysis (Figures 3 and 4).

12  
13 Figure 5 compares the model with a global compilation of  $\Delta^{17}\text{O}(\text{nitrate})$  observations from around the world.  
14 Observations included in Figure 5 include locations where there is enough data to calculate monthly means (McCabe  
15 et al., 2006;Kunasek et al., 2008;Hastings et al., 2003;Kaiser et al., 2007;Michalski et al., 2003;Guha et al.,  
16 2017;Savarino et al., 2013;Ishino et al., 2017b;Savarino et al., 2007;Alexander et al., 2009;He et al., 2018b;Fibiger et  
17 al., 2013;Wang et al., 2014). Figure 6 compares the seasonality in modeled  $\Delta^{17}\text{O}(\text{nitrate})$  to the observations where  
18 samples were collected over the course of approximately one year (McCabe et al., 2006;Kunasek et al., 2008;Kaiser  
19 et al., 2007;Michalski et al., 2003;Guha et al., 2017;Savarino et al., 2013;Ishino et al., 2017b;Savarino et al.,  
20 2007;Alexander et al., 2009). In contrast to Alexander et al. (2009), the model does not significantly underestimate  
21 the  $\Delta^{17}\text{O}(\text{nitrate})$  observations when assuming a bulk ozone isotopic composition ( $\Delta^{17}\text{O}(\text{O}_3)$ ) on the order of 25‰ (see  
22 Figure 2d in Alexander et al. (2009)). The increase in modeled  $\Delta^{17}\text{O}(\text{nitrate})$  is due to increased importance of O<sub>3</sub> in  
23 NO<sub>x</sub> cycling (85% below 1 km) compared to Alexander et al. (2009) (80% below 1 km altitude), and an increase in  
24 the number and fractional importance of nitrate formation pathways that yield relatively high values of  $\Delta^{17}\text{O}(\text{nitrate})$   
25 (red pathways in Fig. 1). Although XO species themselves are only a minor NO oxidation pathway (1%), the addition  
26 of reactive halogen chemistry in the model has altered the relative abundance of O<sub>3</sub> and HO<sub>x</sub> (Sherwen et al., 2016) in

1 such a way as to increase the modeled  $\Delta^{17}\text{O}(\text{NO}_x)$ . The Alexander et al. (2009) study used GEOS-Chem v8-01-01,  
2 which included tropospheric nitrate formation from the  $\text{NO} + \text{OH}$ ,  $\text{N}_2\text{O}_5 + \text{H}_2\text{O}$ , and  $\text{NO}_3 + \text{HC}$  pathways only. An  
3 increased importance of  $\text{N}_2\text{O}_5$  hydrolysis (R4) and additional nitrate formation pathways that yield relatively high  
4 values of  $\Delta^{17}\text{O}(\text{nitrate})$  (R5, R6, R8, and R10) in the present study also explain the increase in modeled  $\Delta^{17}\text{O}(\text{nitrate})$   
5 relative to Alexander et al. (2009). An increase in the average  $A$  value from 0.80 to 0.85 would tend to increase the  
6 calculated  $\Delta^{17}\text{O}(\text{nitrate})$  on the order of 2‰ ( $0.05 \times \Delta^{17}\text{O}(\text{O}_3^*)$ ), suggesting that the increase in the relative importance  
7 of the terminal reactions R4, R5, R6, R8, and R10 explains the majority of the difference between the results presented  
8 here compared to (Alexander et al., 2009). Assuming a value of 35‰ for bulk  $\Delta^{17}\text{O}(\text{O}_3)$  in the model that did not  
9 include reactive halogen chemistry or heterogeneous reactions in cloud water produced good agreement between  
10 modeled and observed  $\Delta^{17}\text{O}(\text{nitrate})$  in Alexander et al. (2009); however, in the current version of the model this bulk  
11 isotopic assumption leads to a model overestimate at nearly all locations (Figure S6). The “cloud chemistry” model  
12 shows somewhat better agreement with the observations ( $R^2 = 0.51$  in Figure 5) compared to the “standard” model  
13 ( $R^2 = 0.48$  in Figure S3). Improved agreement with the observations occurs in the mid- to high-latitudes (Figures 6  
14 and S4) is due to addition of  $\text{N}_2\text{O}_5$  hydrolysis in clouds (Figures 3 and S6).

15  
16 The mean  $\Delta^{17}\text{O}(\text{nitrate})$  value of the observations ( $27.7 \pm 5.0\text{‰}$ ) shown in Figure 5 is not significantly different from  
17 the modeled values at the location of the observations ( $28.6 \pm 4.5\text{‰}$ ); however, the range of  $\Delta^{17}\text{O}(\text{nitrate})$  values of  
18 the observations (10.9 – 40.6‰) is larger than in the model (19.6 – 37.6‰). As previously noted in Savarino et al.  
19 (2007), the maximum observed  $\Delta^{17}\text{O}(\text{nitrate})$  value (40.6‰) is not possible given our isotope assumption for the  
20 terminal oxygen atom of ozone ( $\Delta^{17}\text{O}(\text{O}_3^*) = 39\text{‰}$ ); however, it is theoretically possible given the approximately 2‰  
21 uncertainty in observed  $\Delta^{17}\text{O}(\text{O}_3^*)$ . A value of  $\Delta^{17}\text{O}(\text{nitrate}) = 41\text{‰}$  is possible if  $\Delta^{17}\text{O}(\text{O}_3^*) = 41\text{‰}$  and all oxygen  
22 atoms of nitrate originate from ozone ( $A = 1$  and all nitrate forms from R2 and/or R5). Although this may be possible  
23 for nitrate formed locally in the Antarctic winter due to little to no sunlight, lack of local  $\text{NO}_x$  sources during Antarctic  
24 winter makes it unlikely that all nitrate observed in Antarctica forms locally. Long-range transport from lower latitudes  
25 and/or the stratosphere likely contributes to nitrate observed in Antarctica during winter (Lee et al., 2014). Observed  
26  $\Delta^{17}\text{O}(\text{nitrate}) > 39\text{‰}$  (in Antarctica) has been suggested to be due to transport of nitrate from the stratosphere (Savarino  
27 et al., 2007), as stratospheric  $\text{O}_3$  is expected to have a higher  $\Delta^{17}\text{O}(\text{O}_3)$  value than ozone produced in the troposphere

1 (Krankowsky et al., 2000; Mauersberger et al., 2001; Lyons, 2001). Indeed, the model underestimates the observations  
2 at Dumont d'Urville (DDU) and the South Pole (both in Antarctica) during winter and spring (Figure 6), when and  
3 where the stratospheric contribution is expected to be most important (Savarino et al., 2007). The model underestimate  
4 in Antarctica may also be due to model underestimates of BrO column (Chen et al., 2017) and ozone abundance  
5 (Sherwen et al., 2016) in the southern high latitudes. The largest model overestimates occur at Mt. Lulin, Taiwan  
6 (Figures 5 and 6). Based on nitrogen isotope observations ( $\delta^{15}\text{N}$ ), nitrate at Mt. Lulin is thought to be influenced by  
7 anthropogenic nitrate emitted in polluted areas of mainland China and transported to Mt. Lulin, rather than local nitrate  
8 production (Guha et al., 2017). However, observations of  $\Delta^{17}\text{O}(\text{nitrate})$  in autumn and winter in Beijing suggest much  
9 higher values ( $30.6 \pm 1.8\text{‰}$ ) than was measured at Mt. Lulin ( $15 - 30\text{‰}$  in winter). A potential reason for the model  
10 overestimate of the observed values at Mt. Lulin could be qualitatively explained by transport of nitrate formed in the  
11 free troposphere to this high altitude location, where the high  $\Delta^{17}\text{O}(\text{nitrate})$  producing pathways (R4-R8) should be  
12 negligible due to minimal aerosol surface area for heterogeneous chemistry. Low  $\Delta^{17}\text{O}(\text{nitrate})$  values from nitrate  
13 formed at higher altitudes and transported to Mt. Lulin would not be accounted for in the model since the isotopes are  
14 not transported. The model compares better to the mid-latitude locations close to pollution sources (La Jolla and  
15 Princeton), although the model overestimates wintertime  $\Delta^{17}\text{O}(\text{nitrate})$  in Princeton, NJ, USA by up to 6‰ and  
16 underestimates winter time  $\Delta^{17}\text{O}(\text{nitrate})$  in La Jolla, CA, USA by up to 4‰. The model overestimate at Princeton  
17 during winter could be due to the fact that these are precipitation samples and not ambient aerosol samples, and thus  
18 may reflect nitrate formed at altitudes higher than we are sampling in the model. The underestimate at La Jolla, CA  
19 could be due to underestimates in reactive chlorine chemistry in the model, which would tend to increase  $\Delta^{17}\text{O}(\text{nitrate})$   
20 by increasing nitrate formation by the hydrolysis of halogen nitrates (R6) in this coastal location. The model  
21 underestimates the  $\Delta^{17}\text{O}(\text{nitrate})$  observations at Cape Verde in late summer/early autumn by up to 6‰ (Savarino et  
22 al., 2013). Comparison with results from the steady-state model employed in Savarino et al. (2013) suggests that the  
23 low bias could be due to an underestimate of nitrate formation via  $\text{NO}_3 + \text{DMS}$  (R2). The steady-state model in  
24 Savarino et al. (2013) agreed with observations when R2 represented about one-third of total nitrate formation. The  
25 model results presented here have R2 representing about 15% of total nitrate formation in this season. An  
26 underestimate of the relative importance of R2 could result from a model underestimate of atmospheric DMS  
27 abundances.

Formatted: Font: Symbol

Formatted: Superscript

1

## 2 **4. Model uncertainties**

3 The uncertainty in the two most important nitrate formation pathways,  $\text{NO}_2 + \text{OH}$  and  $\text{N}_2\text{O}_5$  hydrolysis, and their  
4 impacts on  $\text{NO}_x$  and oxidant budgets, have been examined and discussed elsewhere (Macintyre and Evans,  
5 2010;Newsome and Evans, 2017;Holmes et al., 2019). The impacts of the formation and hydrolysis of halogen nitrates  
6 on global  $\text{NO}_x$  and oxidant budgets have also been previously examined (Sherwen et al., 2016). Here we focus on  
7 three additional processes using a set of model sensitivity studies. First, we examine the importance of the third most  
8 important nitrate production pathway on the global scale as predicted by the “standard” model,  $\text{NO}_2$  aerosol uptake  
9 and hydrolysis, and its implications for the global  $\text{NO}_x$ , nitrate, and oxidant budgets. Second, we examine the role of  
10 changing anthropogenic  $\text{NO}_x$  emissions over a 15-year period (2000 to 2015) on the relative importance of the  
11 formation of inorganic nitrate from the hydrolysis of organic nitrates. Finally, we examine the role of aerosol nitrate  
12 photolysis on the relative importance of different nitrate formation pathways. The impact of aerosol nitrate photolysis  
13 on  $\text{NO}_x$  and oxidant budgets has been examined in detail elsewhere (Kasibhatla et al., 2018).

14

### 15 **4.1 Heterogeneous uptake and hydrolysis of $\text{NO}_2$**

16 Heterogeneous uptake of  $\text{NO}_2$  to form  $\text{HNO}_3$  and  $\text{HONO}$  is the third most important nitrate formation pathway in the  
17 “standard” model on the global scale (Figure 1). The reaction probability ( $\gamma_{\text{NO}_2}$ ) measured in laboratory studies ranges  
18 between  $10^{-8}$  to  $10^{-4}$  depending on aerosol chemical composition (Lee and Tang, 1988;Crowley et al., 2010;Gutzwiller  
19 et al., 2002;Yabushita et al., 2009;Abbatt and Waschewsky, 1998;Burkhart et al., 2015;Broske et al., 2003;Li et al.,  
20 2018a;Xu et al., 2018). A value of  $\gamma_{\text{NO}_2} = 10^{-4}$  is used in the “standard” model, which is at the high end of the reported  
21 range. A molar yield of 0.5 for both  $\text{HNO}_3$  and  $\text{HONO}$  formation is assumed in the model based on laboratory studies  
22 and hypothesized reaction mechanisms (Finlayson-Pitts et al., 2003;Jenkin et al., 1988;Ramazan et al., 2004;Yabushita  
23 et al., 2009). However, both the reaction rate and mechanism of this reaction and its dependence on chemical  
24 composition and pH is still not well understood (Spataro and Ianniello, 2014).

25

26 The “cloud chemistry” simulation uses a reaction probability formulation for aerosol uptake of  $\text{NO}_2$  ( $\gamma_{\text{NO}_2}$ ) that  
27 depends on aerosol chemical composition, ranging from  $\gamma_{\text{NO}_2} = 10^{-8}$  for dust to  $\gamma_{\text{NO}_2} = 10^{-4}$  for black carbon based on  
28 recent laboratory studies (Holmes et al., 2019). The updated  $\text{NO}_2$  reaction probability results in a negligible (<1%)

1 importance of this reaction for nitrate formation, compared to 12% contribution in the “standard” model. The “cloud  
2 chemistry” simulation significantly increases the fractional importance of  $\text{N}_2\text{O}_5$  hydrolysis (from 28 to 41%, globally  
3 below 1 km altitude) compared to the “standard” simulation, in part due to decreased competition from  $\text{NO}_2$  hydrolysis  
4 and in part due to increased  $\text{N}_2\text{O}_5$  hydrolysis in clouds. To evaluate the relative importance of competition from  $\text{NO}_2$   
5 hydrolysis and the addition of  $\text{N}_2\text{O}_5$  hydrolysis in clouds, we perform a model sensitivity study that is the same as the  
6 “standard” simulation but decreases the reaction probability of  $\text{NO}_2$  hydrolysis on aerosol ( $\gamma_{\text{NO}_2} = 10^{-7}$ ), without adding  
7  $\text{N}_2\text{O}_5$  hydrolysis in clouds. Similar to the “cloud chemistry” simulation, using  $\gamma_{\text{NO}_2} = 10^{-7}$  renders  $\text{NO}_2$  hydrolysis a  
8 negligible nitrate formation pathway, and increases the relative importance of  $\text{N}_2\text{O}_5$  hydrolysis from 28% to 37%.  
9 This suggests that reduced competition from  $\text{NO}_2$  hydrolysis is the main reason for the increased importance of  $\text{N}_2\text{O}_5$   
10 hydrolysis in the “cloud chemistry” simulation, though the addition of heterogeneous reactions on clouds also plays a  
11 role.

12  
13  $\text{NO}_2$  hydrolysis represents a significant source of HONO in the “standard” model simulation; the reduced  $\text{NO}_2$  reaction  
14 probability from  $\gamma_{\text{NO}_2} = 10^{-4}$  to  $\gamma_{\text{NO}_2} = 10^{-7}$  results in a reduction of HONO below 1 km altitude by up to 100% over  
15 the continents, with relatively small (up to 1 ppb) changes in nitrate concentrations (Figure 7). The reduction in the  
16 rate of heterogeneous  $\text{NO}_2$  uptake leads to reductions in OH where this reaction was most important in the model  
17 (over China and Europe) due to reductions in HONO, but leads to increases in OH elsewhere due to increases in ozone  
18 (by up to a few ppb) resulting from small increases in the  $\text{NO}_x$  lifetime due to a reduction in the  $\text{NO}_x$  sink (Figure 8).  
19 Similar changes in HONO are seen when comparing the “standard” and “cloud chemistry” simulation (not shown).  
20 Increased importance of  $\text{N}_2\text{O}_5$  hydrolysis in both the “cloud chemistry” simulation and the simulation without cloud  
21 chemistry but with a reduced reaction probability for  $\text{NO}_2$  hydrolysis increases modeled annual-mean  $\Delta^{17}\text{O}(\text{nitrate})$   
22 by up to 3% in China where this reaction is most important. This improves model agreement with monthly-mean  
23 observations of  $\Delta^{17}\text{O}(\text{nitrate})$  in Beijing (He et al., 2018a) (Figures 5 and S3).

24  
25 The product yields of  $\text{NO}_2$  hydrolysis are also uncertain. Jenkin et al. (1988) proposed the formation of a water  
26 complex,  $\text{NO}_2 \cdot \text{H}_2\text{O}$ , leading to the production of HONO and  $\text{HNO}_3$ . Finlayson-Pitts et al. (2003) and Ramazan et al.  
27 (2004) proposed the formation of the dimer  $\text{N}_2\text{O}_4$  on the surface, followed by isomerization to form  $\text{NO}^+\text{NO}_3^-$ .  
28 Reaction of  $\text{NO}^+\text{NO}_3^-$  with  $\text{H}_2\text{O}$  results in the formation of HONO and  $\text{HNO}_3$ . Laboratory experiments by Yabushita

1 et al. (2009) suggested that dissolved anions catalyzed the dissolution of  $\text{NO}_2$  to form a radical intermediate  $\text{X-NO}_2^\cdot$   
2 (where  $\text{X} = \text{Cl}, \text{Br}, \text{or I}$ ) at the surface followed by reaction with  $\text{NO}_2(\text{g})$  to form HONO and  $\text{NO}_3^\cdot$ . These experiments  
3 described above were performed at  $\text{NO}_2$  concentrations much higher than exist in the atmosphere (10 – 100 ppm)  
4 (Yabushita et al., 2009; Finlayson-Pitts et al., 2003; Ramazan et al., 2004). A laboratory study utilizing isotopically  
5 labeled water to investigate the reaction mechanism suggested that the formation of HONO resulted from the reaction  
6 between adsorbed  $\text{NO}_2$  and  $\text{H}^+$ , while the formation of  $\text{HNO}_3$  resulted from the reaction between adsorbed  $\text{NO}_2$  and  
7  $\text{OH}^-$ , and did not involve the  $\text{N}_2\text{O}_4$  intermediate (Gustafsson et al., 2009). Results from Gustafsson et al. (2009)  
8 suggest an acidity-dependent yield of HONO and  $\text{HNO}_3$ , favoring HONO at low pH values. A recent study in the  
9 northeast U.S. during winter found that modeled nitrate abundance was overestimated using a molar yield of 0.5 for  
10 HONO and  $\text{HNO}_3$ , and the model better matched the observations of  $\text{NO}_2$  and nitrate when assuming a molar yield of  
11 1.0 for HONO (Jaeglé et al., 2018). Particles were acidic ( $\text{pH} < 2$ ) during this measurement campaign (Guo et al.,  
12 2017; Shah et al., 2018), which may favor HONO production over  $\text{HNO}_3$ .

13  
14 We examine the potential importance of this acidity-dependent yield by implementing a pH-dependent product yield  
15 in two separate sensitivity simulations, first using an  $\text{NO}_2$  aerosol uptake reaction probability of  $\gamma = 10^{-4}$  as in the  
16 “standard” simulation and second with  $\gamma_{\text{NO}_2} = 10^{-7}$ . The acidity-dependent yield for HONO and  $\text{HNO}_3$  formation is  
17 based on the laboratory study by Gustafsson et al. (2009). We use aerosol pH calculated from ISORROPIA II  
18 (Fountoukis and Nenes, 2007) to calculate the concentration of  $[\text{H}^+]$  and  $[\text{OH}^-]$  in aerosol water. The yield of HONO  
19 ( $Y_{\text{HONO}}$ ) from heterogeneous uptake of  $\text{NO}_2$  on aerosol surfaces is calculated according to E3:

$$20 \quad Y_{\text{HONO}} = \frac{[\text{H}^+]}{[\text{H}^+] + [\text{OH}^-]} \quad (\text{E3})$$

21 where  $[\text{H}^+]$  and  $[\text{OH}^-]$  are in units of M. The yield of  $\text{HNO}_3$  from this reaction is equal to  $(1 - Y_{\text{HONO}})$ . E3 yields values  
22 of  $Y_{\text{HONO}}$  near unity for aerosol pH values less than 6, decreasing rapidly to zero between pH values between 6-8  
23 (Figure S8). Calculated aerosol pH values are typically  $< 6$  in the model except in remote regions far from  $\text{NO}_x$   
24 sources (Figure S9), favoring the product HONO.

25  
26 The acidity-dependent yield implemented in the “standard” simulation with  $\gamma_{\text{NO}_2} = 10^{-4}$  increases HONO  
27 concentrations by up to 1 ppbv in China where this reaction is most important (Figure 9). Fractional increases in  
28 HONO exceed 100% in remote locations (Figure 9). Increased HONO leads to increases in OH on the order of 10 –

1 20% in most locations below 1 km altitude, while ozone concentrations increase in most locations by up to several  
2 ppbv (Figure 9). The exception is the southern high latitudes; likely due to decreased formation and thus transport of  
3 nitrate to remote locations. The impact on NO<sub>x</sub> and nitrate budgets is relatively minor. The global, annual mean NO<sub>x</sub>  
4 burden near the surface (below 1 km) increases slightly (+2%) as a result of the decreased rate of conversion of NO<sub>2</sub>  
5 to nitrate; the change to the global tropospheric burden is negligible. Annual-mean surface nitrate concentrations  
6 show small decreases up to 1 ppbv in China where this reaction is most important in the model; impacts on nitrate  
7 concentrations over a shorter time period may be more significant (Jaeglé et al., 2018). The fraction of HNO<sub>3</sub> formed  
8 from NO<sub>2</sub> + OH (49%) increases due to increases in OH from the HONO source. The fraction of HNO<sub>3</sub> formation  
9 from the uptake and hydrolysis of N<sub>2</sub>O<sub>5</sub> also increases (from 28% to 32%) due to reductions in the nighttime source  
10 of nitrate from NO<sub>2</sub> hydrolysis. The calculated mean  $\Delta^{17}\text{O}(\text{nitrate})$  at the location of the observations shown in Figure  
11 5 ( $27.9 \pm 5.0\%$ ) is not significantly impacted due to compensating effects from changes in both high- and low-  
12 producing  $\Delta^{17}\text{O}(\text{nitrate})$  values. Modeled monthly mean  $\Delta^{17}\text{O}(\text{nitrate})$  in China, where NO<sub>2</sub> hydrolysis is most  
13 important ~~de~~creases by ~~-10.9-1.9%~~, ~~but and is still~~ biased low by ~~+21.8-3.4%~~.

14  
15 Using a combination of both the low reaction probability ( $\gamma = 10^{-7}$ ) and the acidity-dependent yield gives similar results  
16 as using  $\gamma = 10^{-7}$  and assuming a molar yield of 0.5 for HONO and HNO<sub>3</sub> (not shown). In other words, including a  
17 pH-dependent product yield rather than a yield of 0.5 for HONO and nitrate results in negligible differences for  
18 oxidants, NO<sub>x</sub> and nitrate abundances when the reaction probability ( $\gamma_{\text{NO}_2}$ ) is low.

19

#### 20 **4.2 Hydrolysis of organic nitrates (RONO<sub>2</sub>)**

21 Anthropogenic NO<sub>x</sub> emissions have been increasing in China and decreasing in the U.S. and Europe (Richter et al.,  
22 2005;Hoesly et al., 2018b), with implications for the relative importance of inorganic and organic nitrate formation as  
23 a sink for NO<sub>x</sub> (Zare et al., 2018). To examine the impacts of recent changes in anthropogenic NO<sub>x</sub> emissions for  
24 nitrate formation pathways, we run the “standard” model using the year 2000 emissions and meteorology after a 1-  
25 year model spin up, and compare the results to the “standard” model simulation run in the year 2015. This time-period  
26 encompasses significant changes in anthropogenic NO<sub>x</sub> emissions in the U.S., Europe, and China, and encompasses  
27 most of the time period of the observations shown in Figures 5 and 6. Total, global anthropogenic emissions of NO<sub>x</sub>  
28 are slightly lower in the 2000-year simulation (30 Tg N yr<sup>-1</sup>) compared to the year 2015 simulation (31 Tg N yr<sup>-1</sup>) due

1 to decreases in North America and Europe, counteracted by increases in Asia (Figure S10). This leads to increases of  
2 less than 10% in the annual-mean, fractional importance of the source of nitrate from the hydrolysis of organic nitrates  
3 in the U.S., and corresponding decreases of less than 10% over China (Figure 10). Relatively small changes (< 10%)  
4 in nitrate formation pathways yield small changes (< 2‰) in modeled annual-mean  $\Delta^{17}\text{O}(\text{nitrate})$  between the year  
5 2000 and 2015, differences in  $\Delta^{17}\text{O}(\text{nitrate})$  over shorter time periods may be larger. Changes in the formation of  
6 nitrate from the hydrolysis of  $\text{RONO}_2$  remains unchanged globally, as increases in the U.S. and Europe and decreases  
7 in China counteract one another.

8

#### 9 **4.3 Photolysis of aerosol nitrate**

10 Observations have demonstrated that aerosol nitrate can be photolyzed at rates much faster than  $\text{HNO}_3(\text{g})$  (Reed et al.,  
11 2017;Ye et al., 2016); however, the magnitude of the photolytic rate constant is uncertain. We examine the  
12 implications of this process for global nitrate formation pathways by implementing the photolysis of aerosol nitrate as  
13 described in Kasibhatla et al. (2018) into the “standard” model simulation, scaling the photolytic rate constant for both  
14 fine- and coarse-mode aerosol nitrate to a factor of 25 times higher than that for  $\text{HNO}_3(\text{g})$  (Kasibhatla et al.,  
15 2018;Romer et al., 2018), with a molar yield of 0.67 for HONO and 0.33 for  $\text{NO}_x$  production. The global, annual  
16 mean  $\text{NO}_x$  burden near the surface (below 1 km) increases slightly (+2%) as a result of the photolytic recycling of  
17 nitrate to  $\text{NO}_x$ , similar to Kasibhatla et al. (2018). Aerosol nitrate photolysis results in only small impacts on the  
18 relative importance of nitrate formation pathways (< 2%) likely due to simultaneous increases in  $\text{O}_3$  and OH  
19 (Kasibhatla et al., 2018), which in turn yields small impacts on calculated  $\Delta^{17}\text{O}(\text{nitrate})$  at the location of the  
20 observations shown in Figure 5 ( $27.9 \pm 5.0\text{‰}$ ). Nitrate photolysis itself has minimal impact on  $\Delta^{17}\text{O}(\text{nitrate})$  because  
21 it is a mass-dependent process (McCabe et al., 2005).

22

#### 23 **5 Conclusions**

24 Observations of  $\Delta^{17}\text{O}(\text{nitrate})$  can be used to help quantify the relative importance of different nitrate formation  
25 pathways. Interpretation of  $\Delta^{17}\text{O}(\text{nitrate})$  requires knowledge of  $\Delta^{17}\text{O}(\text{O}_3)$ . Previous modeling studies showed good  
26 agreement between observed and modeled  $\Delta^{17}\text{O}(\text{nitrate})$  when assuming a bulk oxygen isotopic composition of ozone  
27 ( $\Delta^{17}\text{O}(\text{O}_3)$ ) of 35‰ based on laboratory and modeling studies (Morton et al., 1990;Thiemens, 1990;Lyons, 2001).  
28 However, recent and spatially widespread observations of  $\Delta^{17}\text{O}(\text{O}_3)$  have consistently shown  $\Delta^{17}\text{O}(\text{O}_3) = 26 \pm 1\text{‰}$ ,

1 suggesting that models are underestimating the role of ozone relative to HO<sub>x</sub> in NO<sub>x</sub> chemistry. We utilize a global  
2 compilation of observations of  $\Delta^{17}\text{O}(\text{nitrate})$  to assess the representation of nitrate formation in a global chemical  
3 transport model (GEOS-Chem), assuming that the bulk oxygen isotopic composition of ozone ( $\Delta^{17}\text{O}(\text{O}_3) = 26\%$ ).  
4 The modeled  $\Delta^{17}\text{O}(\text{nitrate})$  is roughly consistent with observations, with a mean modeled and observed  $\Delta^{17}\text{O}(\text{nitrate})$   
5 of  $(28.6 \pm 4.5\%)$  and  $(27.6 \pm 5.0\%)$ , respectively, at the locations of the observations. Improved agreement between  
6 modeled and observed  $\Delta^{17}\text{O}(\text{nitrate})$  is due to increased importance of ozone versus HO<sub>2</sub> and RO<sub>2</sub> in NO<sub>x</sub> cycling and  
7 an increase in the number and importance of nitrate production pathways that yield high  $\Delta^{17}\text{O}(\text{nitrate})$  values. The  
8 former may be due to implementation of tropospheric reactive halogen chemistry in the model, which impacts ozone  
9 and HO<sub>x</sub> abundances. The latter is due mainly to increases in the relative importance of N<sub>2</sub>O<sub>5</sub> hydrolysis, with the  
10 hydrolysis of halogen nitrates also playing an important role in remote regions.

11  
12 The main nitrate formation pathways in the model below 1 km altitude are from NO<sub>2</sub> + OH and N<sub>2</sub>O<sub>5</sub> hydrolysis (both  
13 41%). The relative importance of global nitrate formation from the hydrolysis of halogen nitrates and hydrogen-  
14 abstraction reactions involving the nitrate radical (NO<sub>3</sub>) are of similar magnitude (~5%). The formation of nitrate  
15 from the hydrolysis of organic nitrate has increased slightly in the U.S. and decreased in China (changes <10%) due  
16 to changing NO<sub>x</sub> emissions from the year 2000 to 2015, although the global mean fractional importance (6%) remains  
17 unchanged as the regional changes counteract one another. Nitrate formation via heterogeneous NO<sub>2</sub> and NO<sub>3</sub> uptake  
18 and NO<sub>2</sub> + HO<sub>2</sub> are negligible (<2%). Although aerosol nitrate photolysis has important implications for O<sub>3</sub> and OH,  
19 the impacts on nitrate formation pathways are small.

20  
21 The model parameterization for heterogeneous uptake of NO<sub>2</sub> has significant impacts on HONO and oxidants (OH  
22 and ozone) in the model. HONO production from this reaction has been suggested to be an important source of OH  
23 in Chinese haze due to high NO<sub>x</sub> and aerosol abundances (Hendrick et al., 2014; Tong et al., 2016; Wang et al., 2017),  
24 with implications for the gas-phase formation of sulfate aerosol from the oxidation of sulfur dioxide by OH (Shao et  
25 al., 2019; Li et al., 2018b). More recent laboratory studies suggest that the reaction probability of NO<sub>2</sub> on aerosols is  
26 lower than that previously used in the model. Using an NO<sub>2</sub> reaction probability formulation that depends on the  
27 chemical composition of aerosols as described in Holmes et al. (2019) renders this reaction negligible for nitrate  
28 formation, and has significant implications for modeled HONO, ozone, and OH. Although uncertainty also exists in

1 the relative yield of nitrate and HONO from this reaction, the impacts of this assumption are negligible when we use  
2 these updated NO<sub>2</sub> reaction probabilities. Observations of  $\Delta^{17}\text{O}$ (nitrate) in Chinese haze events during winter (He et  
3 al., 2018b) may help to quantify the importance of this nitrate production pathway in a region where the model predicts  
4 it is significant.

5

6 Data availability: The GEOS-Chem model is available at <http://acmg.seas.harvard.edu/geos>.

7

8 Author contributions: B.A. designed the study and performed the model simulations and calculations. All other  
9 authors provided model code and contributed to writing and analysis.

10

11 Competing interests: The authors declare that they have no conflict of interest.

12

### 13 Acknowledgements:

14 B.A. acknowledges NSF AGS 1644998 and 1702266 and helpful discussions with Joël Savarino and Ron Cohen.

15 C.D.H. acknowledges the NASA New Investigator Program grant NNX16AI57G. J.A.F. acknowledges Australian  
16 Research Council funding DP160101598.

17

### 18 References

19 Abbatt, J. P. D., and Waschewsky, G. C. G.: Heterogeneous interactions of OHBr, HNO<sub>3</sub>, O<sub>3</sub>, and NO<sub>2</sub> with  
20 deliquescent NaCl aerosols at room temperature, *J. Phys. Chem. A*, **102**, 3719-3725, 1998.

21 Alexander, B., Savarino, J., Kreutz, K. J., and Thiemens, M. H.: Impact of preindustrial biomass-burning  
22 emissions on the oxidation pathways of tropospheric sulfur and nitrogen, *J. Geophys. Res.*, **109**, D08303,  
23 doi: 10.1029/2003JD004218, 2004.

24 Alexander, B., Hastings, M. G., Allman, D. J., Dachs, J., Thornton, J. A., and Kunasek, S. A.: Quantifying  
25 atmospheric nitrate formation pathways based on a global model of the oxygen isotopic composition  
26 ( $\Delta^{17}\text{O}$ ) of atmospheric nitrate, *Atmos. Chem. Phys.*, **9**, 5043-5056, 10.5194/acp-9-5043-2009, 2009.

27 Atkinson, R.: Atmospheric chemistry of VOCs and NO<sub>x</sub>, *Atm. Env.*, **34**, 2063-2101, 10.1016/S1352-  
28 2310(99)00460-4, 2000.

29 Berhanu, T. A., Savarino, J., Bhattacharya, S. K., and Vicars, W. C.: <sup>17</sup>O excess transfer during the NO<sub>2</sub> + O<sub>3</sub>  
30 --> NO<sub>3</sub> + O<sub>2</sub> reaction, *J. Chem. Phys.*, **136**, 044311, doi: 10.1063/1.3666852, 2012.

31 Bertram, T. H., and Thornton, J. A.: Toward a general parameterization of N<sub>2</sub>O<sub>5</sub> reactivity on aqueous  
32 particles: the competing effects of particle liquid water, nitrate and chloride, *Atmos. Chem. Phys.*, **9**,  
33 8351-8363, 10.5194/acp-9-8351-2009, 2009.

1 Bey, I., Jacob, D. J., Yantosca, R. M., Logan, J. A., Field, B. D., Fiore, A. M., Li, Q., Liu, H. Y., Mickley, L. J.,  
2 and Schultz, M. G.: Global modeling of tropospheric chemistry with assimilated meteorology: Model  
3 description and evaluation, *J. Geophys. Res.*, **106**, 23073-23095, 2001.

4 Bhattacharya, S. K., Pandey, A., and Savarino, J.: Determination of intramolecular isotope distribution of  
5 ozone by oxidation reaction with silver metal, *J. Geophys. Res.*, **113**, D03303, doi:10.1029/2006JF008309,  
6 2008.

7 Bhattacharya, S. K., Savarino, J., Michalski, G., and Liang, M.-C.: A new feature in the internal heavy  
8 isotope distribution in ozone, *J. Chem. Phys.*, **141**, 10.1063/1.4895614, 2014.

9 Brenninkmeijer, C. A. M., Janssen, C., Kaiser, J., Rockmann, T., Rhee, T. S., and Assonov, S. S.: Isotope  
10 effects in the chemistry of atmospheric trace compounds, *Chemical Reviews*, **102**, 5125-5161, 2003.

11 Broske, R., Kleffmann, J., and Wiesen, P.: Heterogeneous conversion of NO<sub>2</sub> on secondary organic  
12 aerosol surfaces: A possible source of nitrous acid (HONO) in the atmosphere?, *Atmos. Chem. Phys.*, **3**,  
13 469-474, 10.5194/acp-3-469-2003, 2003.

14 Brothers, L. A., Dominguez, G., Fabian, P., and Thiemens, M. H.: Using multi-isotope tracer methods to  
15 understand the sources of nitrate in aerosols, fog and river water in Podocarpus National Forest,  
16 Ecuador, *Eos Trans. AGU*, **89**, Abstract A11C-0136, 2008.

17 Browne, E. C., and Cohen, R. C.: Effects of biogenic nitrate chemistry on the NO<sub>x</sub> lifetime in remote  
18 continental regions, *Atmos. Chem. Phys.*, **12**, 11917-11932, 10.5194/acp-12-11917-2012, 2014.

19 Burkhardt, J. F., Sander, S. P., Abbatt, J. P. D., Barker, J. R., Huie, R. E., Kolb, C. E., Kurylo, M. J., Orkin, V. L.,  
20 Wilmoth, D. M., and Wine, P. H.: Chemical Kinetics and Photochemical Data for Use in Atmospheric  
21 Studies, Jet Propulsion Laboratory, Pasadena, CA, USA, 2015.

22 Burkholder, J. B., Sander, S. P., Abbatt, J. P. D., Barker, J. R., Huie, R. E., Kolb, C. E., Kurylo, M. J., Orkin, V.  
23 L., Wilmoth, D. M., and Wine, P. H.: Chemical kinetics and photochemical data for use in atmospheric  
24 studies: evaluation number 18, Jet Propulsion Laboratory, Pasadena, CA, 2015.

25 Butkovskaya, N. I., Kukui, A., Pouvesle, N., and Le Bras, G.: Formation of Nitric Acid in the Gas-Phase HO<sub>2</sub>  
26 + NO Reaction: Effects of Temperature and Water Vapor, *J. Phys. Chem. A*, **109**, 6509-6520,  
27 10.1021/jp051534v, 2005.

28 Chen, Q., Schmidt, J. A., Shah, V., Jaeglé, L., Sherwen, T., and Alexander, B.: Sulfate production by  
29 reactive bromine: Implications for the global sulfur and reactive bromine budgets, *Geophys. Res. Lett.*,  
30 **44**, 7069-7078, 10.1002/2017GL073812, 2017.

31 Chen, Q., Edebeli, J., McNamara, S. M., Kulju, K., May, N. W., Bertman, S. P., Thanekar, S., Fuentes, J. D.,  
32 and Pratt, K. A.: HONO, Particulate Nitrite, and Snow Nitrite at a Midlatitude Urban Site during  
33 Wintertime, *ACS Earth Space Chem.*, 10.1021/acsearthspacechem.9b00023, 2019.

34 Connell, P., and Johnston, H. S.: Thermal dissociation of N<sub>2</sub>O<sub>5</sub> in N<sub>2</sub>, *Geophys. Res. Lett.*, **6**, 553-556,  
35 1979.

36 Costa, A. W., Michalski, G., Schauer, A. J., Alexander, B., Steig, E. J., and Shepson, P. B.: Analysis of  
37 atmospheric inputs of nitrate to a temperate forest ecosystem from  $\Delta^{17}\text{O}$  isotope ratio measurements,  
38 *Geophys. Res. Lett.*, **38**, L15805, doi:10.1029/2011GL047539, 2011.

39 Crowley, J. N., Ammann, M., Cox, R. A., Hynes, R. G., Jenkin, M. E., Mellouki, A., Rossi, M. J., Troe, J., and  
40 Wallington, T. J.: Evaluated kinetic and photochemical data for atmospheric chemistry: Volume V –  
41 heterogeneous reactions on solid substrates, *Atmos. Chem. Phys.*, **10**, 9059-9223, 10.5194/acp-10-9059-  
42 2010, 2010.

43 Domine, F., and Shepson, P. B.: Air-Snow Interactions and Atmospheric Chemistry, *Science*, **297**, 1506,  
44 2002.

45 Dubey, M. K., Mohrschladt, R., Donahue, N. M., and Anderson, J. G.: Isotope-specific kinetics of hydroxyl  
46 radical (OH) with water (H<sub>2</sub>O): Testing models of reactivity and atmospheric fractionation, *J. Phys. Chem.*  
47 *A*, **101**, 1494-1500, 1997.

1 Evans, M. J., and Jacob, D. J.: Impact of new laboratory studies of N<sub>2</sub>O<sub>5</sub> hydrolysis on global model  
2 budgets of tropospheric nitrogen oxides, ozone, and OH, *Geophys. Res. Lett.*, **32**, L09813,  
3 doi:10.1029/2005GL022469, 2005.

4 Ewing, S. A., Michalski, G., Thiemens, M., Quinn, R. C., Macalady, J. L., Kohl, S., Wankel, S. D., Kendall, C.,  
5 McKay, C. P., and Amundson, R.: Rainfall limit of the N cycle on Earth, *Global Biogeochemical Cycles*, **21**,  
6 GB3009, 10.1029/2006gb002838, 2007.

7 Fibiger, D. L., Hastings, M. G., Dibb, J. E., and Huey, L. G.: The preservations of atmospheric nitrate in  
8 snow at Summit, Greenland, *Geophys. Res. Lett.*, **40**, 3484-3489, 10.1002/grl.50659, 2013.

9 Finlayson-Pitts, B. J., Wingen, L. M., Sumner, A. L., Syomin, D., and Ramazan, K. A.: The heterogeneous  
10 hydrolysis of NO<sub>2</sub> in laboratory systems and in outdoor and indoor atmospheres: An integrated  
11 mechanism, *Phys. Chem. Chem. Phys.*, **5**, 223-242, 2003.

12 Fisher, J. A., Jacob, D. J., Travis, K. R., Kim, P. S., Marais, E. A., Miller, C. C., Yu, K., Zhu, L., Yantosca, R. M.,  
13 Sulprizio, M. P., Mao, J., Wennberg, P. O., Crounse, J. D., Teng, A. P., Nguyen, T. B., St. Clair, J. M., Cohen,  
14 R. C., Romer, P., Nault, B. A., Wooldridge, P. J., Jimenez, J. L., Campuzano-Jost, P., D.A., D., Hu, W.,  
15 Shepson, P. B., Wiong, F., Blake, D. R., Goldstein, A. H., Misztal, P. K., Hanisco, T. F., Wolfe, G. M.,  
16 Ryerson, T. B., Wisthaler, A., and Mikoviny, T.: Organic nitrate chemistry and its implications for  
17 nitrogen budgets in an isoprene- and monoterpene-rich atmosphere: constraints from aircraft (SEAC<sup>4</sup>RS)  
18 and ground-based (SOAS) observations in the Southeast US, *Atmos. Chem. Phys.*, **16**, 5969-5991,  
19 10.5194/acp-16-5969-2016, 2016.

20 Fisher, J. A., Atlas, E. L., Barletta, B., Meinardi, S., Blake, D. R., Thompson, C. R., Ryerson, T. B., Peischl, J.,  
21 Tzompa-Sosa, Z. A., and Murray, L. T.: Methyl, Ethyl, and Propyl Nitrates: Global Distribution and Impacts  
22 on Reactive Nitrogen in Remote Marine Environments, *J. Geophys. Res.*, **123**, 429-412,451,  
23 doi.org/10.1029/2018JD029046, 2018.

24 Fountoukis, C., and Nenes, A.: ISORROPIA II: a computationally efficient thermodynamic equilibrium  
25 model for K<sup>+</sup>-Ca<sup>2+</sup>-Mg<sup>2+</sup>-NH<sub>4</sub><sup>+</sup>-Na<sup>+</sup>-SO<sub>4</sub><sup>2-</sup>-NO<sub>3</sub><sup>-</sup>-Cl<sup>-</sup>-H<sub>2</sub>O aerosols, *Atmos. Chem. Phys.*, **7**, 4639-4659, 2007.

26 Geng, L., Cole-Dai, J., Alexander, B., Savarino, J., Schauer, A. J., Steig, E. J., Lin, P., and Zatzko, M. C.: On  
27 the origin of the occasional springtime nitrate concentration maximum in Greenland snow, *Atmos.*  
28 *Chem. Phys. Discuss.*, **14**, 9401-9437, 10.5194/acpd-14-9401-2014, 2014.

29 Geng, L., Murray, L. T., Mickley, L. J., Lin, P., Fu, Q., Schauer, A. J., and Alexander, B.: Isotopic evidence of  
30 multiple controls on atmospheric oxidants over climate transitions, *Nature*, **546**, 133-136,  
31 10.1038/nature22340, 2017.

32 Guha, T., Lin, C. T., Bhattacharya, S. K., Mahajan, A. S., Ou-Yang, C.-F., Lan, Y.-P., Hsu, S. C., and Liang, M.-  
33 C.: Isotopic ratios of nitrate in aerosol samples from Mt. Lulin, a high-altitude station in Central Taiwan,  
34 *Atmos. Env.*, **154**, 53-69, 10.1016/j.atmosenv.2017.01.036, 2017.

35 Guo, H., Weber, R. J., and Nenes, A.: High levels of ammonia do not raise fine particle pH sufficiently to  
36 yield nitrogen oxide-dominated sulfate production, *Scientific Reports*, **7**, 1-7, 10.1038/s41598-017-  
37 11704-0, 2017.

38 Gustafsson, R. J., Kyiakou, G., and Lambert, R. M.: The molecular mechanism of tropospheric nitrous acid  
39 production on mineral dust surfaces, *Chem. Phys. Chem.*, **9**, 1390-1393, 10.1002/cphc.200800259, 2009.

40 Gutzwiller, L., George, C., Rossler, E., and Ammann, J.: Reaction Kinetics of NO<sub>2</sub> with Resorcinol and 2,7-  
41 Naphthalenediol in the Aqueous Phase at Different pH, *J. Phys. Chem. A*, **106**, 12045-12050,  
42 10.1021/jp026240d, 2002.

43 Hastings, M. G., Sigman, D. M., and Lipschultz, F.: Isotopic evidence for source changes of nitrate in rain  
44 at Bermuda, *J. Geophys. Res.*, **108**, 4790, doi:10.1029/2003JD003789, 2003.

45 He, P., Alexander, B., Geng, L., Chi, X., Fan, S., Zhan, H., Kang, H., Zheng, G., Cheng, Y., Su, H., Liu, C., and  
46 Xie, Z.: Isotopic constraints on heterogeneous sulfate production in Beijing haze, *Atmos. Chem. Phys.*, **18**,  
47 5515-5528, 10.5194/acp-18-5515-2018 2018a.

1 He, P., Xie, Z., Chi, X., Yu, X., Fan, S., Kang, H., Liu, C., and Zhan, H.: Atmospheric  $\Delta^{17}\text{O}(\text{NO}_3^-)$  reveals  
2 nocturnal chemistry dominates nitrate production in Beijing haze, *Atmos. Chem. Phys.*, **18**, 14465–14476,  
3 10.5194/acp-18-14465-2018, 2018b.

4 Heidenreich, J. E., and Thiemens, M. H.: A non-mass dependent oxygen isotope effect in the production  
5 of ozone from molecular oxygen: The role of molecular symmetry in isotope chemistry, *J. Chem. Phys.*,  
6 **84**, 2129–2136, 1986.

7 Hendrick, F., Muller, J.-F., Clemer, K., Wang, P., De Maziere, M., Fayt, C., Gielen, C., Hermans, C., Ma, J.,  
8 Z., Pinardi, G., Stavrou, T., Vlemmix, T., and Van Roosendael, M.: Four years of ground-based MAX-  
9 DOAS observations of HONO and  $\text{NO}_2$  in the Beijing area, *Atmos. Chem. Phys.*, **14**, 765–781, 10.5194/acp-  
10 14-765-2014, 2014.

11 Hoesly, R. M., Smith, S. J., Feng, L., Klimont, Z., Janssens-Maenhout, G., Pitkanen, T., Seibert, J. J., Vu, L.,  
12 Andres, R. J., Bolt, R. M., Bond, T. C., Dawidowski, L., Kholod, N., Kurokawa, J.-I., Li, M., Liu, L., Lu, Z.,  
13 Moura, M. C. P., O'Rourke, P. R., and Zhang, Q.: Historical (1750–2014) anthropogenic emissions of  
14 reactive gases and aerosols from the Community Emissions Data System (CEDS), *Geosci. Model Dev.*, **11**,  
15 369–408, 10.5194/gmd-11-369-2018, 2018a.

16 Hoesly, R. M., Smith, S. J., Feng, L., Klimont, Z., Janssens-Maenhout, G., Pitkanen, T., Seibert, J. J., Vu, L.,  
17 Andres, R. J., Bolt, R. M., Bond, T. C., Dawidowski, L., Kholod, N., Kurokawa, J., Li, M., Liu, L., Lu, Z.,  
18 Moura, M. C. P., O'Rourke, P. R., and Zhang, Q.: Historical (1750–2014) anthropogenic emissions of  
19 reactive gases and aerosols from the Community Emissions Data System (CEDS), *Geosci. Model Dev.*, **11**,  
20 369–408, 10.5194/gmd-11-369-2018, 2018b.

21 Holmes, C. D., Prather, M. J., and Vinken, G. C. M.: The climate impact of ship  $\text{NO}_x$  emissions: an  
22 improved estimate accounting for plume chemistry, *Atmos. Chem. Phys.*, **14**, 6801–6812, 10.5194/acp-  
23 14-6801-2014, 2014.

24 Holmes, C. D., Bertram, T. H., Confer, K. L., Graham, K. A., Ronan, A. C., Wirks, C. K., and Shah, V.: The  
25 role of clouds in the tropospheric  $\text{NO}_x$  cycle: a new modeling approach for cloud chemistry and its global  
26 implications, *Geophys. Res. Lett.*, **46**, GL081990, 10.1029/2019GL081990, 2019.

27 Horowitz, L. W., Fiore, A. M., Milly, G. P., Cohen, R. C., Perring, A., Wooldridge, P. J., Hess, P. G.,  
28 Emmons, L. K., and Lamarque, J.-F.: Observational constraints on the chemistry of isoprene nitrates over  
29 the eastern United States, *J. Geophys. Res.*, **112**, D12S08, doi:10.1029/2006JD007747, 2007.

30 Hudman, R. C., Moore, N. E., Martin, R. V., Russell, A. R., Mebust, A. K., Valin, L. C., and Cohen, R. C.: A  
31 mechanistic model of global soil nitric oxide emissions: implementation and space based-constraints,  
32 *Atmos. Chem. Phys.*, **12**, 7779–7795, 10.5194/acp-12-7779-2012, 2012.

33 Ishino, S., Hattori, S., Savarino, J., Jourdain, B., Preunkert, S., Legrand, M., Caillon, N., Barbero, A.,  
34 Kuribayashi, K., and Yoshida, N.: Seasonal variations of triple oxygen isotopic compositions of  
35 atmospheric sulfate, nitrate, and ozone at Dumont d'Urville, coastal Antarctica, *Atmos. Chem. Phys.*, **17**,  
36 3713–3727, 10.5194/acp-17-3713-2017, 2017a.

37 Ishino, S., Hattori, S., Savarino, J., Jourdain, B., Preunkert, S., Legrand, M., Caillon, N., Barbero, A.,  
38 Kuribayashi, K., and Yoshida, N.: Seasonal variations of triple oxygen isotopic compositions of  
39 atmospheric sulfate, nitrate, and ozone at Dumont d'Urville, coastal Antarctica, *Atmos. Chem. Phys.*, **17**,  
40 3713–3727, 10.5194/acp-17-3713-2017, 2017b.

41 Jacob, D. J.: Heterogeneous chemistry and tropospheric ozone, *Atmos. Env.*, **34**, 2131–2159, 2000.

42 Jacobs, M. I., Burke, W. J., and Elrod, M. J.: Kinetics of the reactions of isoprene-derived hydroxynitrates:  
43 gas phase epoxide formation and solution phase hydrolysis,, *Atmos. Chem. Phys.*, **2014**, 8933–8946,  
44 10.5194/acp-14-8933-2014, 2014.

45 Jaeglé, L., Steinberger, L., Martin, R. V., and Chance, K.: Global partitioning of  $\text{NO}_x$  sources using satellite  
46 observations: Relative roles of fossil fuel combustion, biomass burning and soil emissions, *Faraday*  
47 *Discussions*, **130**, 407–423, DOI: 10.1039/b502128f, 2005.

1 Jaeglé, L., Shah, V., Thornton, J. A., Lopez-Hilfiker, F. D., Lee, B. H., McDuffie, E. E., Fibiger, D., Brown, S.  
2 S., Veres, P., Sparks, T. L., Ebben, C. J., Wooldridge, P. J., Kenagy, H. S., Cohen, R. C., Weinheimer, A. J.,  
3 Campos, T. L., Montzka, D. D., Digangi, J. P., Wolfe, G. M., Hanisco, T., Schroder, J. C., Campuzano-Jost,  
4 P., Day, D. A., Jimenez, J. L., Sullivan, A. P., Guo, H., and Weber, R. J.: Nitrogen oxides emissions,  
5 chemistry, deposition, and export over the Northeast United States during the WINTER aircraft  
6 campaign, *J. Geophys. Res.*, **123**, 12,368–312,393, doi.org/10.1029/2018JD029133, 2018.  
7 Jenkin, M. E., Cox, R. A., and Williams, D. J.: Laboratory studies of the kinetics of formation of nitrous  
8 acid from the thermal reaction of nitrogen dioxide and water vapor, *Atm. Env.*, **22**, 487-498, 1988.  
9 Johnston, J. C., and Thiemens, M. H.: The isotopic composition of tropospheric ozone in three  
10 environments, *J. Geophys. Res.*, **102**, 25395-25404, 1997.  
11 Kaiser, J., Hastings, M. G., Houlton, B. Z., Rockmann, T., and Sigman, D. M.: Triple Oxygen Isotope  
12 Analysis of Nitrate Using the Denitrifier Method and Thermal Decomposition of N<sub>2</sub>O, *Anal. Chem.*, **79**,  
13 599-607, 2007.  
14 Kasibhatla, P., Sherwen, T., Evans, M. J., Carpenter, L. J., Reed, C., Alexander, B., Chen, Q., Sulprizio, M.  
15 P., Lee, J. D., Read, K. A., Bloss, W. J., Crilley, L. R., Keene, W. C., Pzenny, A. A. P., and Hodzic, H.: Global  
16 impact of nitrate photolysis of sea-salt aerosol on NO<sub>x</sub>, OH and ozone in the marine boundary layer,  
17 *Atmos. Chem. Phys.*, **18**, 11185-11203, 10.5194/acp-18-11185-2018 2018.  
18 Krankowsky, D., Bartecki, F., Klees, G. G., Mauersberger, K., Schellenback, K., and Stehr, J.: Measurement  
19 of heavy isotope enrichment in tropospheric ozone, *Geophys. Res. Lett.*, **22**, 1713-1716, 1995.  
20 Krankowsky, D., Lammerzahl, P., and Mauersberger, K.: Isotopic measurements of stratospheric ozone,  
21 *Geophys. Res. Lett.*, **27**, 2593-2595, 2000.  
22 Kunasek, S. A., Alexander, B., Hastings, M. G., Steig, E. J., Gleason, D. J., and Jarvis, J. C.: Measurements  
23 and modeling of  $\Delta^{17}\text{O}$  of nitrate in a snowpit from Summit, Greenland, *J. Geophys. Res.*, **113**, D24302,  
24 10.1029/2008JD010103, 2008.  
25 Lee, C., Martin, R. V., van Donkelaar, A., Lee, H., Dickerson, R. R., Hains, J. C., Krotkov, N., Richter, A.,  
26 Innikov, K., and Schwab, J. J.: SO<sub>2</sub> emissions and lifetimes: Estimates from inverse modeling using in situ  
27 and global, space-based (SCIAMACHY and OMI) observations, *J. Geophys. Res.*, **116**, D06304,  
28 10.1029/2010JD014758, 2011.  
29 Lee, H.-M., Henze, D. K., Alexander, B., and Murray, L. T.: Investigating the sensitivity of surface-level  
30 nitrate seasonality in Antarctica to primary sources using a global model, *Atm. Env.*, **89**, 757-767,  
31 10.1016/j.atmosenv.2014.03.003, 2014.  
32 Lee, J. H., and Tang, I. N.: Accommodation coefficient of gaseous NO<sub>2</sub> on water surfaces, *Atm. Env.*, **22**,  
33 1988.  
34 Levy, H., Moxim, W. J., Klonecki, A. A., and Kasibhatla, P. S.: Simulated tropospheric NO<sub>x</sub>: Its evaluation,  
35 global distribution and individual source contributions, *J. Geophys. Res.*, **104**, 26,279-226,306, 1999.  
36 Li, L., Duan, Z., Li, H., Zhu, C., Henkelman, G., Francisco, J. S., and Zeng, X. C.: Formation of HONO from  
37 the NH<sub>3</sub>-promoted hydrolysis  
38 of NO<sub>2</sub> dimers in the atmosphere, *Proc. Natl. Acad. Sci.*, **115**, 7236–7241, 10.1073/pnas.1807719115,  
39 2018a.  
40 Li, L., Hoffmann, M. R., and Colussi, A. J.: Role of Nitrogen Dioxide in the Production of Sulfate during  
41 Chinese Haze-Aerosol Episodes, *Env. Sci. & Tech.*, **52**, 2686-2693, 10.1021/acs.est.7b05222, 2018b.  
42 Li, M., Q. Zhang, J. Kurokawa, J. H. Woo, K. B. He, Z. Lu, T. Ohara, Y. Song, D. G. Streets, G. R. Carmichael,  
43 Y. F. Cheng, C. P. Hong, H. Huo, X. J. Jiang, S. C. Kang, F. Liu, H. Su, and Zheng, B.: MIX: a mosaic Asian  
44 anthropogenic emission inventory for the MICS-Asia and the HTAP projects, *Atmos. Chem. Phys.*, **17**,  
45 935-963, 10.5194/acp-17-935-2017, 2017.

1 Liang, J., Horowitz, L. W., Jacob, D. J., Wang, Y., Fiore, A. M., Logan, J. A., Gardner, G. M., and Munger, J.  
2 W.: Seasonal budgets of reactive nitrogen species and ozone over the United States, and export fluxes to  
3 the global atmosphere,, *J. Geophys. Res.*, 103, 13435–13450,, 1998.  
4 Liu, H., Jacob, D. J., Bey, I., and Yantosca, R. M.: Constraints from  $^{210}\text{Pb}$  and  $^7\text{Be}$  on wet deposition and  
5 transport in a global three-dimensional chemical tracer model driven by assimilated meteorological  
6 fields, *J. Geophys. Res.*, 106, 12,109-112,128, 2001.  
7 Long, M. S., Keene, W. C., Easter, R. C., Sander, R., Liu, X., Kerkweg, A., and Erickson, D.: Sensitivity of  
8 tropospheric chemical composition to halogen-radical chemistry using a fully coupled size-resolved  
9 multiphase chemistry-global climate system: halogen distributions, aerosol composition, and sensitivity  
10 of climate-relevant gases, *Atmos. Chem. Phys*, 14, 3397-3425, 10.5194/acp-14-3397-2014, 2014.  
11 Lyons, J. R.: Transfer of mass-independent fractionation on ozone to other oxygen-containing molecules  
12 in the atmosphere, *Geophys. Res. Lett.*, 28, 3231-3234, 2001.  
13 Macintyre, H. L., and Evans, M. J.: Sensitivity of a global model to the uptake of  $\text{N}_2\text{O}_5$  by tropospheric  
14 aerosol, *Atmos. Chem. Phys*, 10, 7409-7401, 10.5194/acp-10-7409-2010, 2010.  
15 Martin, R. V., Jacob, D. J., Yantosca, R. M., Chin, M., and Ginoux, P.: Global and regional decreases in  
16 tropospheric oxidants from photochemical effects of aerosols, *J. Geophys. Res.*, 108, 4097, doi:  
17 4010.1029/2002JD002622, 2003.  
18 Mauersberger, K., Lämmerzahl, P., and Krankowsky, D.: Stratospheric Ozone Isotope Enrichments—  
19 Revisited, *Geophys. Res. Lett.*, 28, 3155-3158, 2001.  
20 McCabe, J. R., Boxe, C. S., Colussi, A. J., Hoffmann, M. R., and Thiemens, M. H.: Oxygen isotopic  
21 fractionation in the photochemistry of nitrate in water and ice, *J. Geophys. Res.*, 110, D15310, 2005.  
22 McCabe, J. R., Savarino, J., Alexander, B., Gong, S., and Thiemens, M. H.: Isotopic constraints on non-  
23 photochemical sulfate production in the Arctic winter, *Geophys. Res. Lett.*, 33, L05810,  
24 10.1029/2005GL025164, 2006.  
25 McCabe, J. R., Thiemens, M. H., and Savarino, J.: A record of ozone variability in South Pole Antarctic  
26 snow: Role of nitrate oxygen isotopes, *J. Geophys. Res.*, 112, D12303, doi:10.1029/2006JD007822, 2007.  
27 Michalski, G., and Bhattacharya, S. K.: The role of symmetry in the mass independent isotope effect in  
28 ozone, *Proc. Natl. Acad. Sci.*, 106, 5493-5496, 2009.  
29 Michalski, G., Bhattacharya, S. K., and Girsch, G.:  $\text{NO}_x$  cycle and the tropospheric ozone isotope  
30 anomaly: an experimental investigation, *Atmos. Chem. Phys*, 14, 4935-4953, 10.5194/acp-14-4935-2014,  
31 2014.  
32 Michalski, G. M., Scott, Z., Kabling, M., and Thiemens, M. H.: First measurements and modeling of  $\Delta^{17}\text{O}$   
33 in atmospheric nitrate, *Geophys. Res. Lett.*, 30, 1870, doi:10.1029/2003GL017015, 2003.  
34 Morin, S., Savarino, J., Bekki, S., Gong, S., and Bottenheim, J. W.: Signature of Arctic surface ozone  
35 depletion events in the isotope anomaly ( $\Delta^{17}\text{O}$ ) of atmospheric nitrate, *Atmos. Chem. Phys.*, 6, 6255-  
36 6297, 2007.  
37 Morin, S., Savarino, J., Frey, M. M., Yan, N., Bekki, S., Bottenheim, J. W., and Martins, J. M. F.: Tracing the  
38 Origin and Fate of  $\text{NO}_x$  in the Arctic Atmosphere Using Stable Isotopes in Nitrate, *Science*, 322, 730-732,  
39 10.1126/science.1161910, 2008.  
40 Morin, S., Savarino, J., Frey, M. M., Dominé, F., Jacobi, H.-W., Kaleschke, L., and Martins, J. M. F.:  
41 Comprehensive isotopic composition of atmospheric nitrate in the Atlantic Ocean boundary layer from  
42 65S to 79N, *J. Geophys. Res.*, 114, D05303, doi:10.1029/2008JD010696, 2009.  
43 Morin, S., Sander, R., and Savarino, J.: Simulation of the diurnal variations of the oxygen isotope  
44 anomaly ( $\Delta^{17}\text{O}$ ) of reactive atmospheric species, *Atmos. Chem. Phys*, 11, 3653-3671, doi:10.5194/acp-  
45 11-3653-2011, 2011.  
46 Morton, J., Barnes, J., Schueler, B., and Mauersberger, K.: Laboratory studies of heavy ozone, *J. Geophys.*  
47 *Res.*, 95, 901-907, 1990.

1 Müller, J.-F., Peeters, J., and Stavrou, T.: Fast photolysis of carbonyl nitrates from isoprene, *Atmos.*  
2 *Chem. Phys.*, **14**, 2497–2508, 10.5194/acp-14-2497-2014, 2014.

3 Murray, L. T., Jacob, D. J., Logan, J. A., Hudman, R. C., and Koshak, W. J.: Optimized regional and  
4 interannual variability of lightning in a global chemical transport model constrained by LIS/OTD satellite  
5 data, *J. Geophys. Res.*, **117**, D20307, 10.1029/2012JD017934, 2012.

6 Murray, L. T.: Lightning NO<sub>x</sub> and Impacts on Air Quality, *Curr. Pollution Rep.*, **2**, 115–133,  
7 10.1007/s40726-016-0038-0, 2016.

8 Newsome, B., and Evans, M. J.: Impact of uncertainties in inorganic chemical rate constants on  
9 tropospheric composition and ozone radiative forcing, *Atmos. Chem. Phys.*, **17**, 14333–14352,  
10 10.5194/acp-17-14333-2017, 2017.

11 O'Brien, J., Shepson, P., Muthuramu, K., Hao, C., Niki, H., Hastie, D., Taylor, R., and Roussel, P.:  
12 Measurements of alkyl and multifunctional organic nitrates at a rural site in Ontario, *J. Geophys. Res.*,  
13 **100**, 22795–22804, 1995.

14 Park, R. J., Jacob, D. J., Field, B. D., Yantosca, R. M., and Chin, M.: Natural and transboundary pollution  
15 influences on sulfate-nitrate-ammonium aerosols in the United States: implications for policy, *J.*  
16 *Geophys. Res.*, **109**, D15204, 10.1029/2003JD004473, 2004.

17 Parrella, J. P., Jacob, D. J., Liang, Q., Zhang, Y., Mickley, L. J., Miller, B., Evans, M. J., Yang, X., Pyle, J. A.,  
18 Theys, N., and Roozendaal, M. V.: Tropospheric bromine chemistry: implications for present and pre-  
19 industrial ozone and mercury, *Atmos. Chem. Phys.*, **12**, 6723–6740, 10.5194/acp-12-6723-2012, 2012.

20 Paulot, F., Crouse, J. D., Kjaergaard, H. G., Kroll, J. H., Seinfeld, J. H., and Wennberg, P. O.: Isoprene  
21 photooxidation: new insights into the production of acids and organic nitrates, *Atmos. Chem. Phys.*, **9**,  
22 1479–1501, 2009.

23 Ramazan, K. A., Syomin, D., and Finlayson-Pitts, B. J.: The photochemical production of HONO during the  
24 heterogeneous hydrolysis of NO<sub>2</sub>, *Phys. Chem. Chem. Phys.*, **6**, 3836–3843, 10.1039/b402195a, 2004.

25 Reed, C., Evans, M. J., Crilley, L. R., Bloss, W. J., Sherwen, T., Read, K. A., Lee, J. D., and Carpenter, L.:  
26 Evidence for renoxification in the tropical marine boundary layer, *Atmos. Chem. Phys.*, **17**, 4081–4092,  
27 10.5194/acp-17-4081-2017, 2017.

28 Richter, A., Borrows, J. P., Nub, H., Granier, C., and Niemier, U.: Increase in tropospheric nitrogen dioxide  
29 over China observed from space, *Nature*, **437**, 129–132, 10.1038/nature04092, 2005.

30 Rindelaub, J. D., McAvey, K. M., and Shepson, P. B.: The photochemical production of organic nitrates  
31 from  $\alpha$ -pinene and loss via acid-dependent particle phase hydrolysis, *Atmos. Environ.*, **193**–201,  
32 10.1016/j.atmosenv.2014.11.010, 2015.

33 Romer, P. S., Wooldridge, P. J., Crouse, J. D., Kim, M. J., Wennberg, P. O., Dibb, J. E., Scheuer, E., Blake,  
34 D. R., Meinardi, S., Brosius, A. L., Thames, A. B., Miller, D. O., Brune, W. H., Hall, S. R., Ryerson, T. B., and  
35 Cohen, R. C.: Constraints on Aerosol Nitrate Photolysis as a Potential Source of HONO and NO<sub>x</sub>,  
36 *Environmental Science & Technology*, **52**, 13738–13746, 10.1021/acs.est.8b03861, 2018.

37 Saiz-Lopez, A., Lamarque, J. F., Kinnison, D. E., Tilmes, S., Ordóñez, C., Orlando, J. J., Conley, A. J., Plane,  
38 J. M. C., Mahajan, A. S., Sousa Santos, G., Atlas, E. L., Blake, D. R., Sander, S. P., Schauffler, S., Thompson,  
39 A. M., and Brasseur, G. P.: Estimating the climate significance of halogen-driven ozone loss in the  
40 tropical marine troposphere, *Atmos. Chem. Phys.*, **12**, 3939–3949, 10.5194/acp-12-3939-2012, 2012.

41 Savarino, J., and Thiemens, M. H.: Analytical procedure to determine both  $\delta^{18}\text{O}$  and  $\delta^{17}\text{O}$  of H<sub>2</sub>O<sub>2</sub> in  
42 natural water and first measurements, *Atmos. Environ.*, **33**, 3683–3690, 1999b.

43 Savarino, J., Kaiser, J., Morin, S., Sigman, D. M., and Thiemens, M. H.: Nitrogen and oxygen isotopic  
44 constraints on the origin of atmospheric nitrate in coastal Antarctica, *Atmos. Chem. Phys.*, **7**, 1925–1945,  
45 2007.

46 Savarino, J., Bhattacharya, S. K., Morin, S., Baroni, M., and Doussin, J.-F.: The NO+O<sub>3</sub> reaction: A triple  
47 oxygen isotope perspective on the reaction dynamics and atmospheric implications for the transfer of  
48 the ozone isotope anomaly, *J. Chem. Phys.*, **128**, 194303, 10.1063/1.2917581, 2008.

1 Savarino, J., Morin, S., Erbland, J., Grannec, F., Patey, M., Vicars, W., Alexander, B., and Achterberg, E. P.:  
2 Isotopic composition of atmospheric nitrate in a tropical marine boundary layer, PNAS, published ahead  
3 of print, doi:10.1073/pnas.1216639110, 2013.

4 Schmidt, J. A., Jacob, D. J., Horowitz, H. M., Hu, L., Sherwen, T., Evans, M. J., Liang, Q., Sulieman, R. M.,  
5 Oram, D. E., Le Breton, M., Percival, C. J., Wang, S., Dix, B., and Volkamer, R.: Modeling the observed  
6 tropospheric BrO background: Importance of multiphase chemistry and implications for ozone, OH, and  
7 mercury, *J. Geophys. Res.*, 121, 11,819-811,835, 10.1002/2015JD024229, 2016.

8 Shah, V., Jaeglé, L., Thornton, J. A., Lopez-Hilfiker, F. D., Lee, B. H., Schroder, J. C., Campuzano-Jost, P.,  
9 Jimenez, J. L., Guo, H., Sullivan, A. P., Weber, R. J., Green, J. R., Fiddler, M. N., Bililign, S., Campos, T. L.,  
10 Stell, M., Weinheimer, A. J., Montzka, D. D., and Brown, S. S.: Chemical feedbacks weaken the  
11 wintertime response of particulate sulfate and nitrate to emissions reductions over the eastern United  
12 States, *Proc. Natl. Acad. Sci.*, 115, 8110-8115, 10.1073/pnas.1803295115, 2018.

13 Shao, J., Chen, Q., Wang, Y., Xie, Z., He, P., Sun, Y., Lu, X., Shah, V., Martin, R. V., Philip, S., Song, S., Zhao,  
14 Y., Zhang, L., and Alexander, B.: Heterogeneous sulfate aerosol formation mechanisms during  
15 wintertime Chinese haze events: Air quality model assessment using observations of sulfate oxygen  
16 isotopes in Beijing, *Atmos. Chem. Phys.*, 19, 6107-6123, 10.5194/acp-19-6107-2019, 2019.

17 Sharma, H. D., Jervis, R. E., and Wing, K. Y.: Isotopic exchange reactions in nitrogen oxides, *J. Phys.*  
18 *Chem.*, 74, 923-933, 1970.

19 Sherwen, T., Schmidt, J. A., Evans, M. J., Carpenter, L. J., Brobmann, K., Eastham, S. D., Jacob, D. J., Dix,  
20 B., Koenig, T. K., Sinreich, R., Ortega, I. K., Volkamer, R., Saiz-Lopez, A., Prados-Roman, C., Mahajan, A. S.,  
21 and Ordóñez, C.: Global impacts of tropospheric halogens (Cl, Br, I) on oxidants and composition in  
22 GEOS-Chem, *Atmos. Chem. Phys.*, 16, 12239-12271, 10.5194/acp-16-12239-2016, 2016.

23 Sherwen, T., Evans, M. J., Sommariva, R., Hollis, L. D. J., Ball, S. M., Monks, P. S., Reed, C., Carpenter, L. J.,  
24 Lee, J. D., Forster, G., Bandy, B., Reeves, C. E., and Bloss, W. J.: Effects of halogens on European air-  
25 quality, *Faraday Discuss.*, 200, 75-100, 10.1039/C7FD00026J, 2017.

26 Singh, H. B., Herlth, D., O'Hara, D., Zahnle, K., Bradshaw, J. D., Sandholm, S. T., Talbot, R., Crutzen, P. J.,  
27 and Kanakidou, M.: Relationship of Peroxyacetyl nitrate to active and total odd nitrogen at northern  
28 high latitudes: Influence of reservoir species on NO<sub>x</sub> and O<sub>3</sub>, *J. Geophys. Res.*, 97, 16,523-516,530, 1992.

29 Sofen, E. D., Alexander, B., Steig, E. J., Thiemens, M. H., Kunasek, S. A., Amos, H. M., Schauer, A. J.,  
30 Hastings, M. G., Bautista, J., Jackson, T. L., Vogel, L. E., McConnell, J. R., Pasteris, D. R., and Saltzman, E.  
31 S.: WAIS Divide ice core suggests sustained changes in the atmospheric formation pathways of sulfate  
32 and nitrate since the 19th century in the extratropical Southern Hemisphere, *Atmos. Chem. Phys.*, 14,  
33 5749-5769, 10.5194/acp-14-5749-2014, 2014.

34 Spataro, F., and Ianniello, A.: Sources of atmospheric nitrous acid: State of the science, current research  
35 needs, and future prospects, *Journal of the Air and Waste Management Association*, 64, 1232-1250,  
36 10.1080/10962247.2014.952846, 2014.

37 Stettler, M. E. J., Eastham, S., and Barrett, S. R. H.: Air quality and public health impacts of UK airports.  
38 Part I: Emissions, *Atm. Env.*, 45, 5415-5424, 10.1016/j.atmosenv.2011.07.012, 2011.

39 Tan, F., Tong, S., Jing, B., Hou, S., Liu, Q., Li, K., Zhang, Y., and Ge, M.: Heterogeneous reactions of NO<sub>2</sub>  
40 with CaCO<sub>3</sub>-(NH<sub>4</sub>)<sub>2</sub>SO<sub>4</sub> mixtures at different relative humidities, *Atmos. Chem. Phys.*, 16, 8081-8093,  
41 10.5194/acp-16-8081-2016, 2016.

42 Thiemens, M. H., T. Jackson: Pressure dependency for heavy isotope enhancement in ozone formation,  
43 *Geophys. Res. Lett.*, 17, 717-719, 1990.

44 Tong, S. R., Hou, S. Q., Zhang, Y., Chu, B. W., Liu, Y. C., He, H., Zhao, P. S., and Ge, M. F.: Exploring the  
45 nitrous acid (HONO) formation mechanism in winter Beijing: direct emissions and heterogeneous  
46 production in urban and suburban areas, *Faraday Discuss.*, 189, 213-230, 10.1039/c5fd00163c, 2016.

1 Vicars, W., and Savarino, J.: Quantitative constraints on the  $^{17}\text{O}$ -excess ( $\Delta^{17}\text{O}$ ) signature of surface  
2 ozone: Ambient measurements from 50°N to 50°S using the nitrite-coated filter technique, *Geochem.*  
3 *Cosmochem. Acta*, 135, 270-287, 10.1016/j.gca.2014.03.023, 2014.

4 Vicars, W. C., Bhattacharya, S. K., Erbland, J., and Savarino, J.: Measurement of the  $^{17}\text{O}$ -excess ( $\Delta^{17}\text{O}$ ) of  
5 tropospheric ozone using a nitrite-coated filter, *Rapid Commun. Mass Spectrom.*, 26, 1219-1231,  
6 10.1002/rcm.6218, 2012.

7 Vinken, G. C. M., Boersma, K. F., Jacob, D. J., and Meijer, E. W.: Accounting for non-linear chemistry of  
8 ship plumes in the GEOS-Chem global chemistry transport model, *Atmos. Chem. Phys.*, 11, 11707-11722,  
9 10.5194/acp-11-11707-2011, 2011.

10 von Glasow, R., and Crutzen, P. J.: Model study of multiphase DMS oxidation with a focus on halogens,  
11 *Atmos. Chem. Phys.*, 4, 589-608, 2004.

12 Wang, F., Michalski, G., Seo, J., and Ge, W.: Geochemical, isotopic, and mineralogical constraints on  
13 atmospheric deposition in the hyper-arid Atacama Desert, Chile, *Geochem. Cosmochem. Acta*, 135, 29-  
14 48, 10.1016/j.gca.2014.03.017, 2014.

15 Wang, J. Q., Zhang, X. S., Guo, J., Wang, Z. W., and Zhang, M. G.: Observation of nitrous acid (HONO) in  
16 Beijing, China: Seasonal variation, nocturnal formation and daytime budget, *Science of the Total*  
17 *Environment*, 587, 10.1016/j.scitotenv.2017.02.159, 2017.

18 Wang, X., Jacob, D. J., Eastham, S., Sulprizio, M., Zhu, L., Chen, Q., Alexander, B., Sherwen, T., Evans, M.  
19 J., Lee, B. H., Haskins, J., Lopez-Hilfiker, F. D., Thornton, J. A., Huey, L. G., and Liao, H.: The role of  
20 chlorine in tropospheric chemistry, *Atmos. Chem. Phys. Discuss.*, 10.5194/acp-2018-1088, 2018.

21 Wang, Y. H., Jacob, D. J., and Logan, J. A.: Global simulation of tropospheric  $\text{O}_3$ - $\text{NO}_x$  hydrocarbon  
22 chemistry 1. Model formulation, *J. Geophys. Res.*, 103, 713-710,725, 1998.

23 Xu, L., Guo, H., Boyd, C. M., Klein, M., Bougiatioti, A., Cerully, K. M., Hite, J. R., Isaacman-VanWertz, G.,  
24 Kreisberg, N. M., Knote, C., Olson, K., Koss, A., Goldstein, A. H., Hering, S. V., de Gouw, J., Baumann, K.,  
25 Lee, S.-H., Nenes, A., Weber, R. J., and Ng, N. L.: Effects of anthropogenic emissions on aerosol formation  
26 from isoprene and monoterpenes in the southeastern United States, *Proc. Natl. Acad. Sci.*, 112, 37-42,  
27 10.1073/pnas.1417609112, 2015.

28 Xu, W., Kuang, Y., Zhao, C., Tao, J., Zhao, G., Bian, Y., Yu, Y., Shen, C., Liang, L., and Zhang, G.:  $\text{NH}_3$ -  
29 promoted hydrolysis of  $\text{NO}_2$  induces explosive 1 growth in HONO, *Atmos. Chem. Phys. Discuss.*,  
30 <https://doi.org/10.5194/acp-2018-996>, 2018.

31 Yabushita, A., Enami, S., Sakamoto, Y., Kawasaki, M., Hoffman, M. R., and Colussi, A. J.: Anion-Catalyzed  
32 Dissolution of  $\text{NO}_2$  on Aqueous Microdroplets, *J. Phys. Chem. A Lett.*, 113, 4844-4848,  
33 10.1021/jp900685f, 2009.

34 Yang, X., Cox, R. A., Warwick, N. J., Pyle, J. A., Carver, G. C., O'Connor, F. M., and Savage, N. H.:  
35 Tropospheric bromine chemistry and its impact on ozone: A model study, *J. Geophys. Res.*, 110, D2331,  
36 doi:10.1029/2005JD003244, 2005.

37 Ye, C., Zhou, X., Pu, D., Stutz, J., Festa, J., Spolaor, M., Tsai, C., Cantrell, C., Mauldin III, R. L., Campos, T.,  
38 Weinheimer, A., Hornbrook, R. S., Apel, E., Guenther, A., Kaser, L., Yuan, B., Karl, T., Haggerty, J., Hall, S.,  
39 Ullmann, K., Smith, J. N., Ortega, J., and Knote, C.: Rapid cycling of reactive nitrogen in the marine  
40 boundary layer, *Nature*, 532, 489-491, 10.1038/nature17195, 2016.

41 Ye, C., Zhou, X., Pu, D., Stutz, J., Festa, J., Spolaor, M., Tsai, C., Cantrell, C., Mauldin III, R. L., Weinheimer,  
42 A., Hornbrook, R. S., Apel, E. C., Guenther, A., Kaser, L., Yuan, B., Karl, T., Haggerty, J., Hall, S., Ullmann,  
43 K., Smith, J., and Ortega, J.: Tropospheric HONO distribution and chemistry in the southeastern US,  
44 *Atmos. Chem. Phys.*, 18, 9107-9120, 10.5194/acp-18-9107-2018, 2018.

45 Zare, A., Romer, P. S., Nguyen, T., Keutsch, F. N., Skog, K., and Cohen, R. C.: A comprehensive organic  
46 nitrate chemistry: insights into the lifetime of atmospheric organic nitrates, *Atmos. Chem. Phys.*  
47 *Discuss.*, 10.5194/acp-2018-530, 2018.

1 Zhang, L., Gong, S., Padro, J., and Barrie, L.: A size-segregated particle dry deposition scheme for an  
2 atmospheric aerosol module, *Atmos. Env.*, 35, 549-560, 2001.

3

4

5

6

7

8

9

10

11

12

13

14

15

16

17

18

19

20

21

1 **Table 1.** Calculated  $\Delta^{17}\text{O}(\text{nitrate})$  in the model for each nitrate production pathway (X = Br, Cl,  
 2 and I; HC = hydrocarbon; MTN = monoterpene; ISOP = isoprene;  $\Delta^{17}\text{O}(\text{O}_3^*) = 39\text{‰}$ ). A is  
 3 defined in equation E1.

4

	Nitrate formation pathway	$\Delta^{17}\text{O}(\text{nitrate})$
Gas-phase reactions		
R1	$\text{NO}_2 + \text{OH}$	$\frac{2}{3} A \Delta^{17}\text{O}(\text{O}_3^*)$
R2	$\text{NO}_3 + \text{HC}$	$(\frac{2}{3} A + \frac{1}{3}) \Delta^{17}\text{O}(\text{O}_3^*)$
R3	$\text{NO} + \text{HO}_2$	$\frac{1}{3} A \Delta^{17}\text{O}(\text{O}_3^*)$
Aerosol uptake from the gas-phase followed by hydrolysis		
R4	$\text{N}_2\text{O}_5 + \text{H}_2\text{O}_{(\text{aq})}$	$(\frac{2}{3} A + \frac{1}{6}) \Delta^{17}\text{O}(\text{O}_3^*)$
R5	$\text{N}_2\text{O}_5 + \text{Cl}^-(\text{aq})$	$(\frac{2}{3} A + \frac{1}{3}) \Delta^{17}\text{O}(\text{O}_3^*)$
R6	$\text{XNO}_3 + \text{H}_2\text{O}_{(\text{aq})}$	$(\frac{2}{3} A + \frac{1}{3}) \Delta^{17}\text{O}(\text{O}_3^*)$
R7	$\text{NO}_2 + \text{H}_2\text{O}_{(\text{aq})}$	$\frac{2}{3} A \Delta^{17}\text{O}(\text{O}_3^*)$
R8	$\text{NO}_3 + \text{H}_2\text{O}_{(\text{aq})}$	$(\frac{2}{3} A + \frac{1}{3}) \Delta^{17}\text{O}(\text{O}_3^*)$
R9	$\text{RONO}_2 + \text{H}_2\text{O}_{(\text{aq})}$ (where $\text{RONO}_2$ is from $\text{NO} + \text{RO}_2$ )	$\frac{1}{3} A \Delta^{17}\text{O}(\text{O}_3^*)$
R10	$\text{RONO}_2 + \text{H}_2\text{O}_{(\text{aq})}$ (where $\text{RONO}_2$ is from $\text{NO}_3 + \text{MTN/ISOP}$ )	$(\frac{2}{3} A + \frac{1}{3}) \Delta^{17}\text{O}(\text{O}_3^*)$

5

6

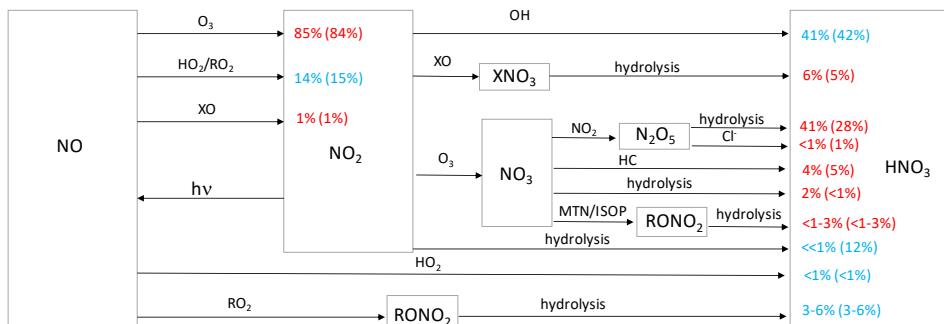
7

8

9

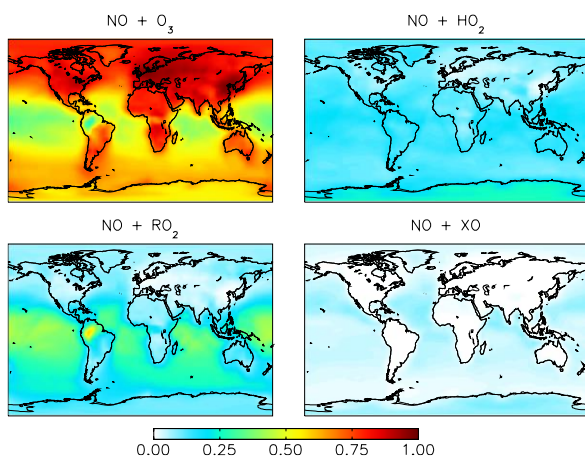
10

11



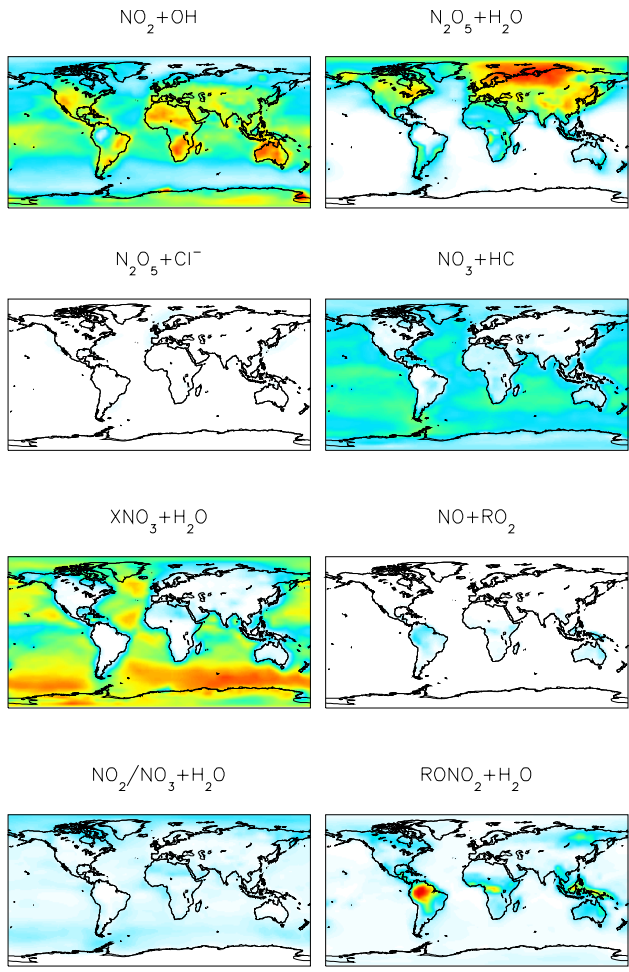
1  
2  
3  
4  
5  
6  
7  
8  
9

**Figure 1.** Simplified HNO<sub>3</sub> formation in the model. Numbers show the global, annual mean percent contribution to NO<sub>2</sub> and HNO<sub>3</sub> formation in the troposphere below 1 km for the “cloud chem” (“standard”) simulation. Red indicates reactions leading to high Δ<sup>17</sup>O values, blue indicates reactions leading to low Δ<sup>17</sup>O values. HO<sub>2</sub> = HO<sub>2</sub>+RO<sub>2</sub>; X = Br+Cl+I; HC = hydrocarbons; MTN = monoterpenes; ISOP = isoprene.

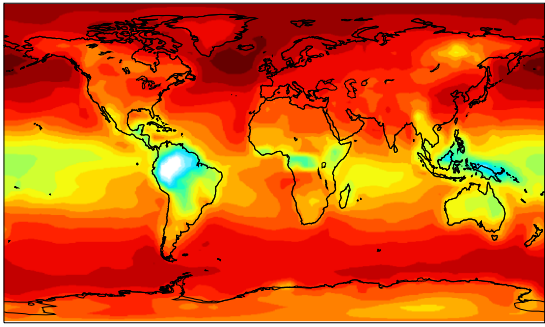


10  
11  
12

**Figure 2.** Annual-mean fraction of NO<sub>2</sub> formation from the oxidation of NO in the troposphere below 1 km altitude in the “cloud chemistry” model.



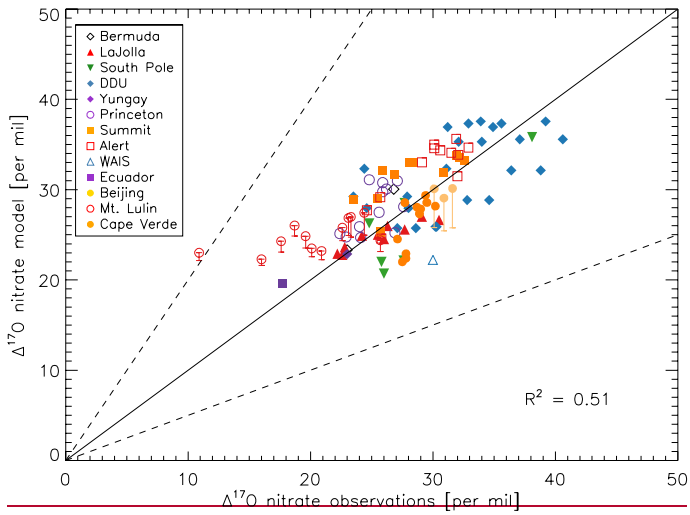
1  
 2 **Figure 3.** Annual-mean fraction of HNO<sub>3</sub> formation from the oxidation of NO<sub>x</sub> in the troposphere below 1  
 3 km altitude in the “cloud chemistry” model.



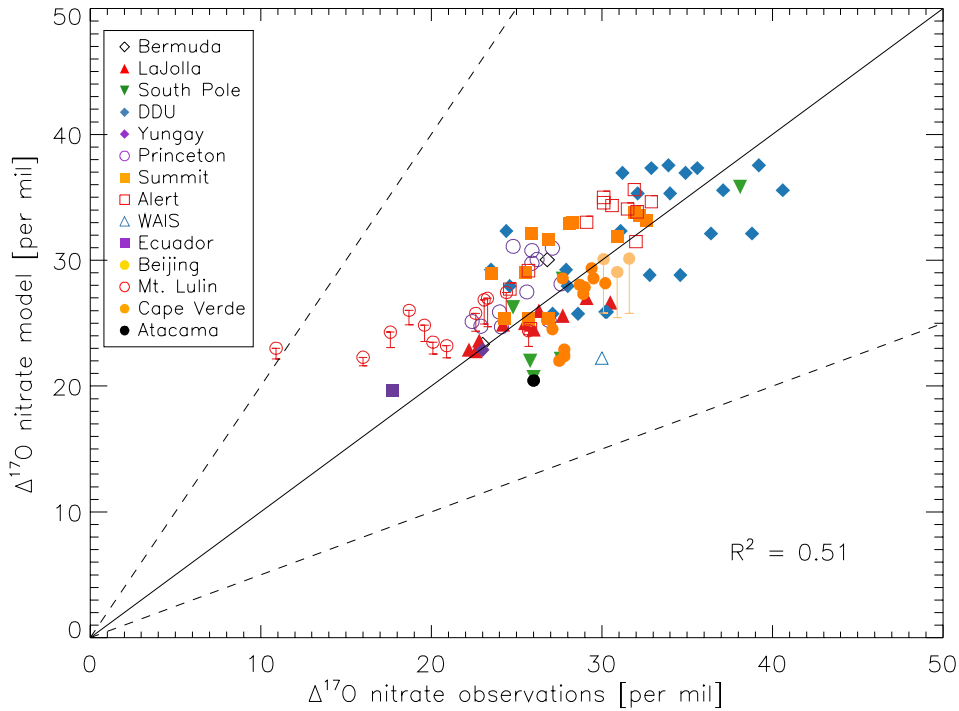
4.0 11.2 18.5 25.8 33.0 [permil]

1  
2  
3  
4  
5

**Figure 4.** Modeled, annual-mean  $\Delta^{17}\text{O}(\text{nitrate})$  below 1 km altitude for the “cloud chemistry” model.



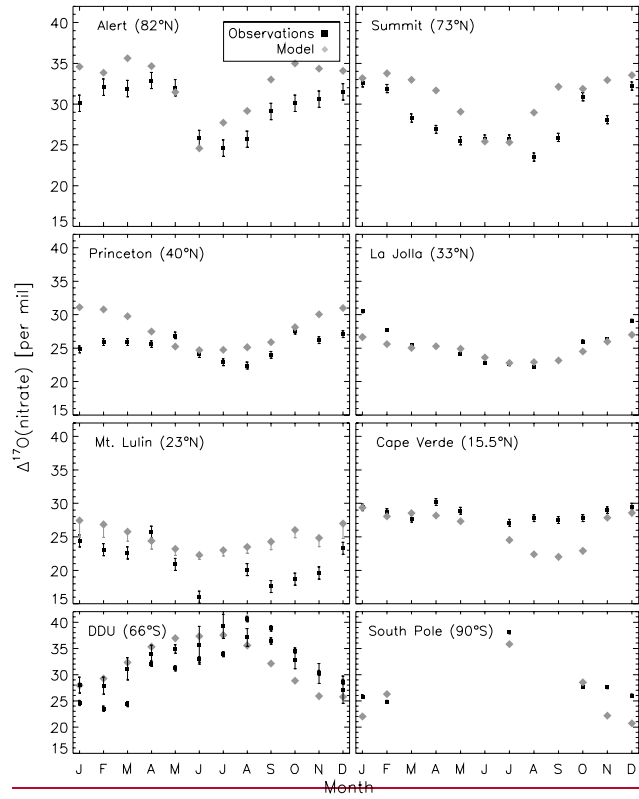
6



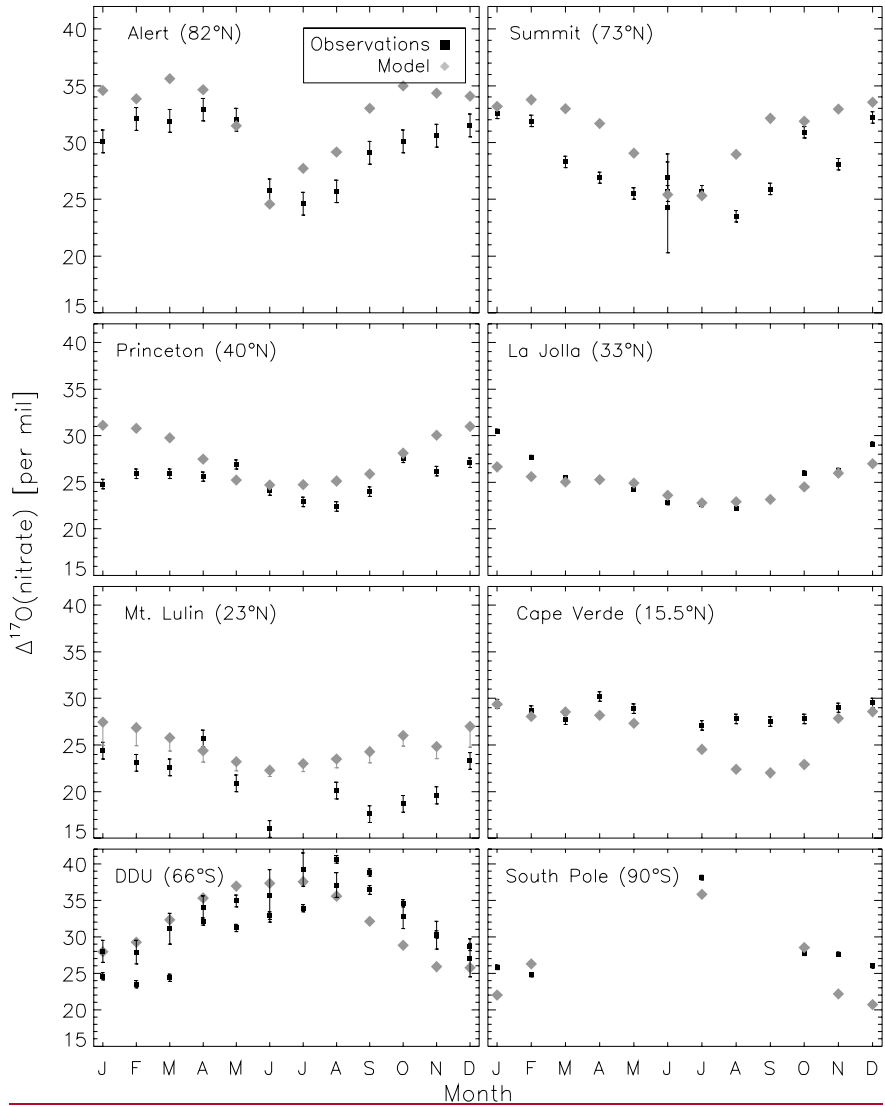
1

2 **Figure 5.** Comparison of monthly-mean modeled (“cloud chemistry”) and observed  $\Delta^{17}\text{O}(\text{nitrate})$  at  
 3 locations where there are enough observations to calculate a monthly mean. References for the  
 4 observations are in the text. The error bars represent different assumptions for calculated modeled A  
 5 values for nighttime reactions as described in the text. Error bars for Beijing and Mt. Lulin reflect the  
 6 range of possible modeled A values for nighttime reactions as described in the text. The  $y=x$  (solid line)  
 7 and  $y = 2x$  and  $y = 0.5x$  (dashed) are shown.

8

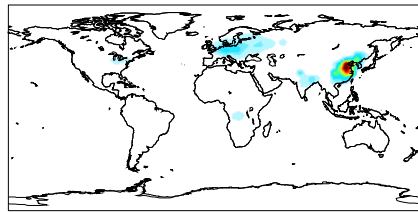


1

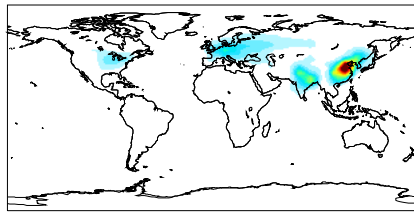


1 **Figure 6.** Comparison of monthly-mean modeled (“cloud chemistry”) and observed  $\Delta^{17}\text{O}(\text{nitrate})$ . Error  
 2 bars for model results from Mt. Lulin reflect the range of possible modeled  $A$  values for nighttime  
 3 reactions as described in the text. Error bars for the observations reflect the analytical uncertainty in the  
 4 measurements, except for two data points in June for Summit which reflect the standard deviation of  
 5  $\Delta^{17}\text{O}(\text{nitrate})$  from multiple measurements during that month.  
 6

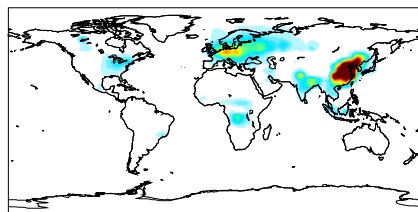
1  
2  
3  
4  
5  
6  
7  
8  
9



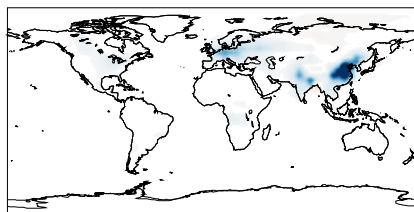
0 500 1000 [pptv]



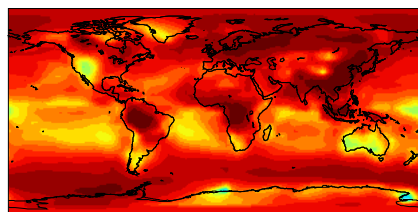
0 5 10 [ppbv]



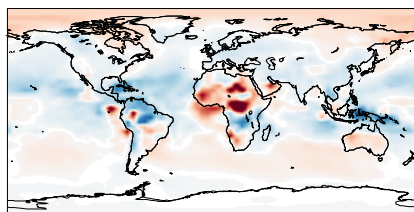
-300 -150 0 [pptv]



-1 0 1 [ppbv]



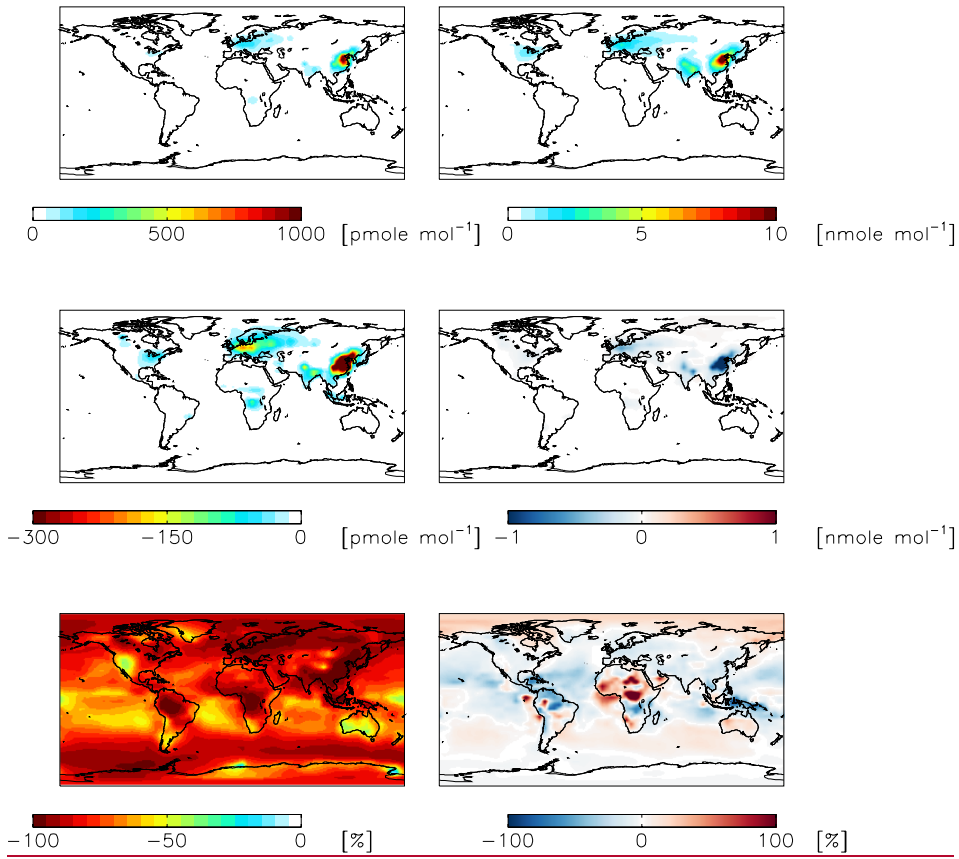
-100 -50 0 [%]



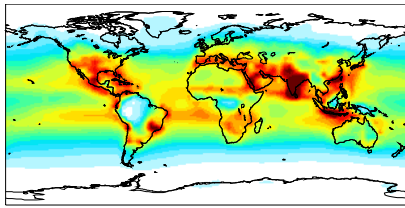
-100 0 100 [%]

1

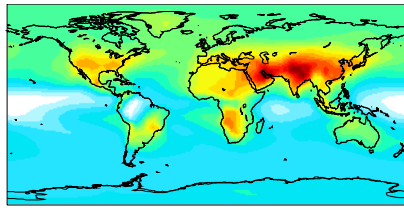
2



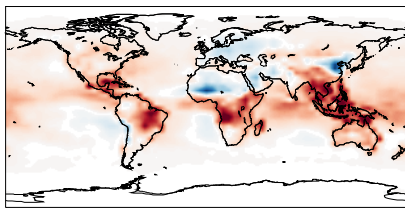
1  
 2 **Figure 7.** Modeled annual-mean HONO (left) and fine-mode nitrate (right) concentrations below 1 km  
 3 altitude in the “standard” simulation (top) with  $\gamma_{\text{NO}_2} = 10^{-4}$  for  $\text{NO}_2$  hydrolysis. Absolute (middle) and  
 4 relative (bottom) change in concentrations below 1 km altitude between the “standard” model and the  
 5 model simulation with  $\gamma_{\text{NO}_2} = 10^{-7}$ . Negative numbers represent a decrease relative to the standard  
 6 simulation.



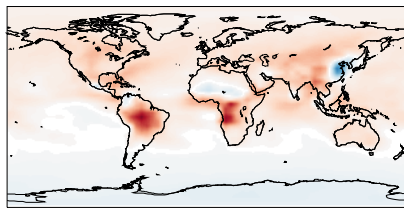
0 50 100 [ $\times 10^5 \text{ cm}^{-3}$ ]



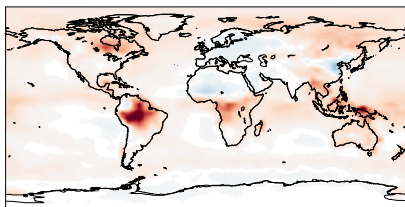
6 35 64 [ppbv]



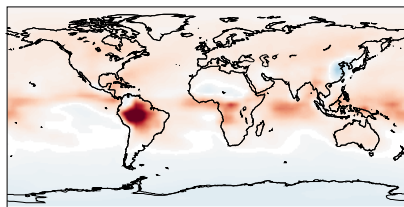
-10 0 10 [ $\times 10^5 \text{ cm}^{-3}$ ]



-7 0 7 [ppbv]

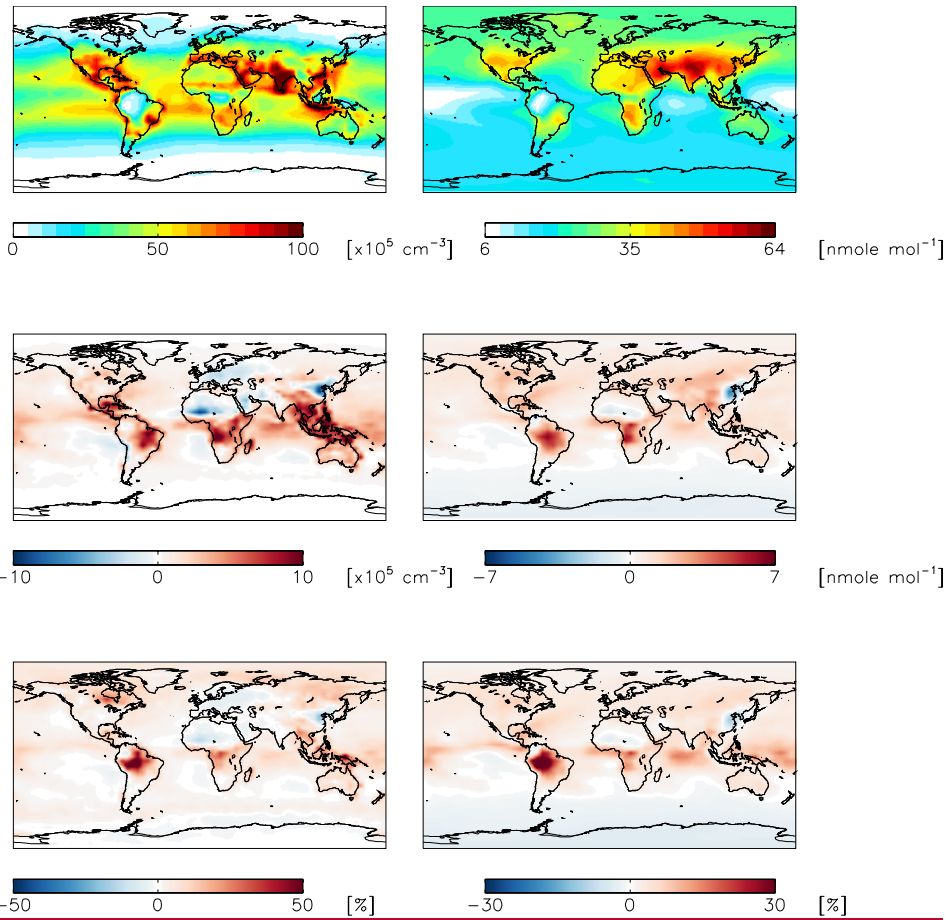


-50 0 50 [%]

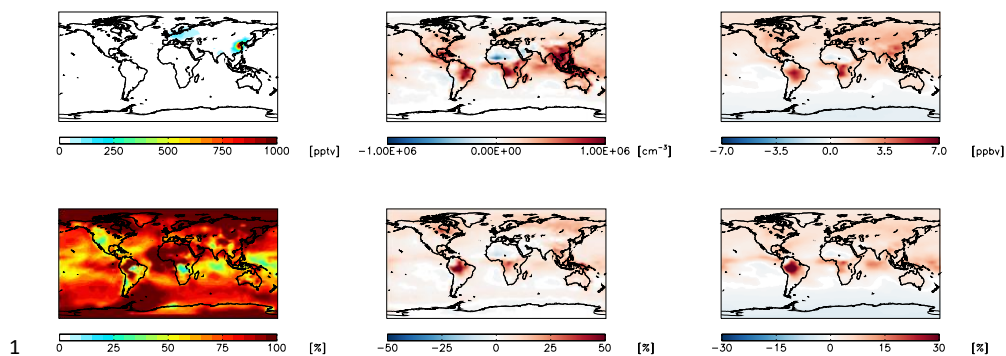


-30 0 30 [%]

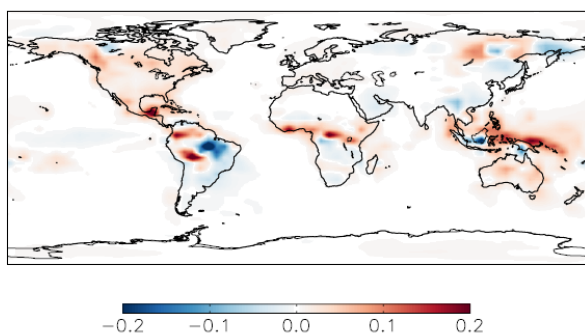
1



1  
2 **Figure 8.** Same as Figure 7 except for OH (left) and ozone (right).  
3



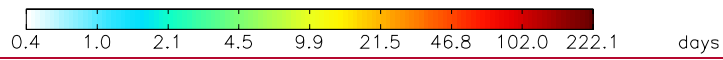
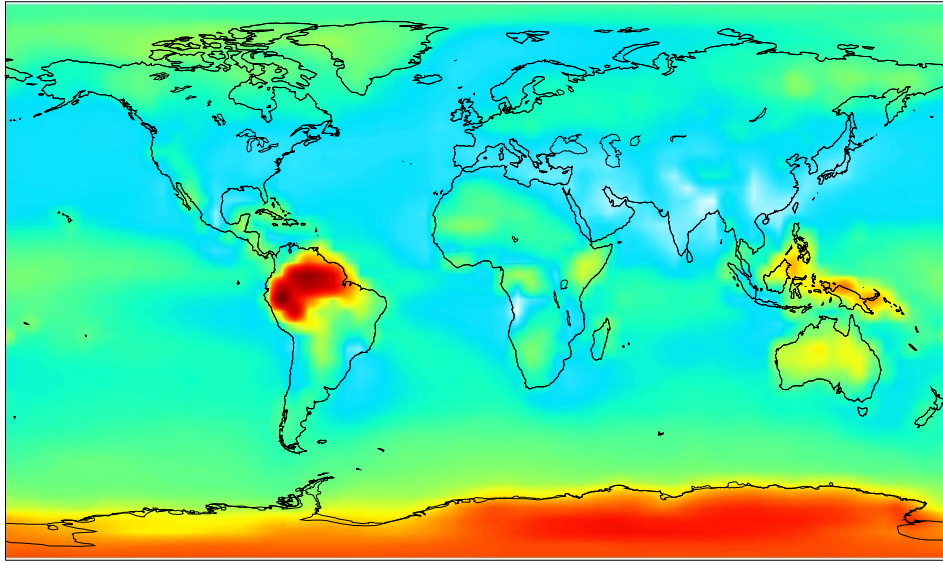
1 **Figure 9.** Absolute (top) and relative (bottom) change in HONO (left), OH (middle), and ozone (right)  
 2 concentrations below 1 km altitude between the “standard” model and the model simulation with an  
 3 acidity-dependent yield from NO<sub>2</sub> hydrolysis. Positive numbers represent an increase relative to the  
 4 “standard” simulation.  
 5



6  
 7 **Figure 10.** Modeled annual-mean difference in the fractional production rate of HNO<sub>3</sub> from the  
 8 hydrolysis of organic nitrate below 1 km altitude in the year 2015 relative to 2000 (2015 - 2000).  
 9

10  
 11  
 12  
 13  
 14  
 15

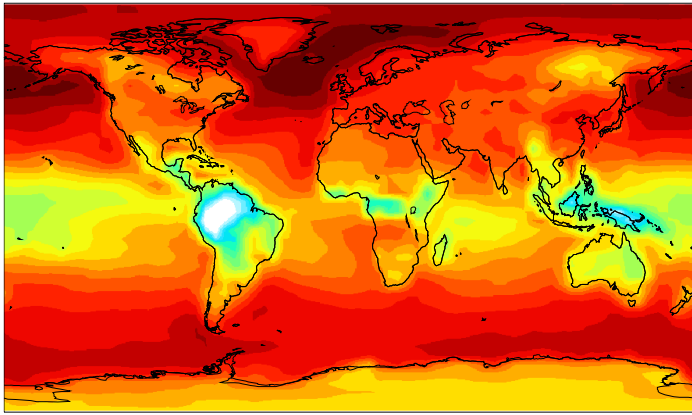
1



2

3 **Figure S1.** Annual mean lifetime of NO<sub>x</sub> below 1 km altitude against oxidation to nitrate via reactions  
4 that occur only at night (R2+R4+R5).

5

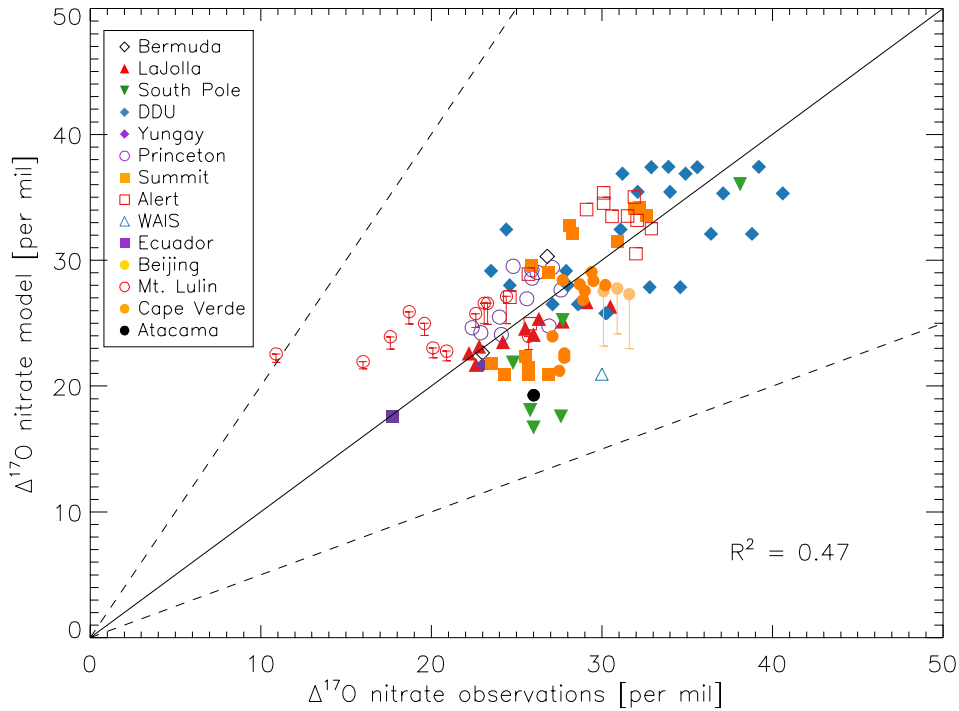


1 4.0 11.2 18.5 25.8 33.0 [permil]

2 **Figure S2.** Same as Figure 4 but for the “standard” simulation.

3

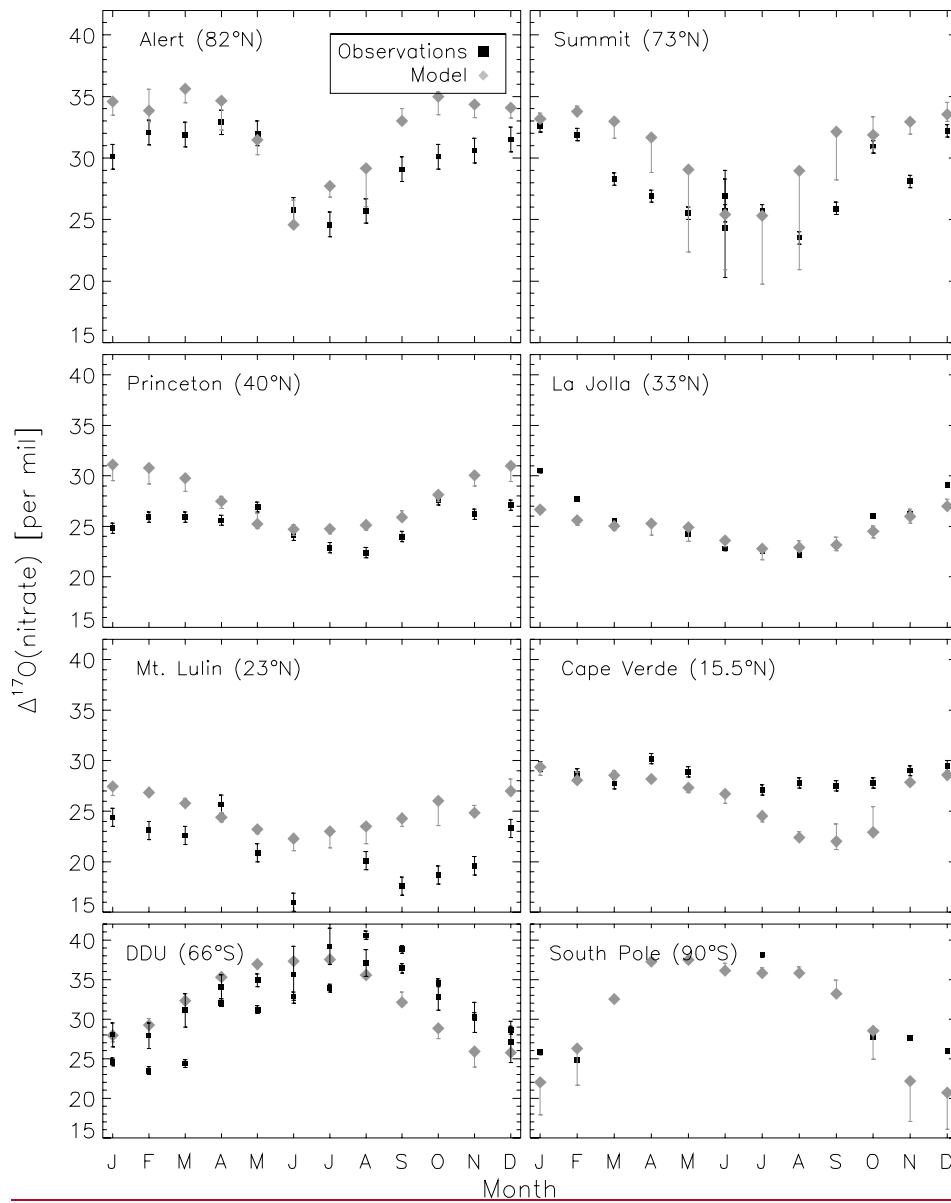
4



1  
2  
3  
4  
5  
6  
7  
8  
9  
10  
11

**Figure S3.**

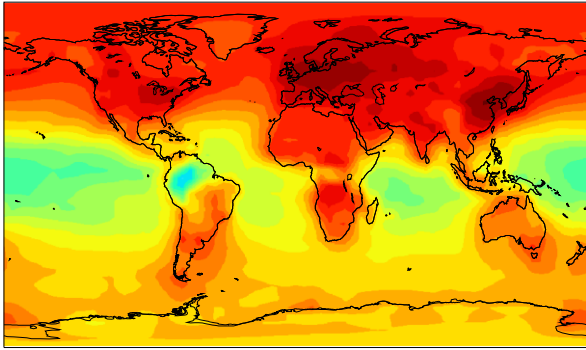
Comparison of monthly-mean modeled (“standard”) and observed  $\Delta^{17}\text{O}$ (nitrate) at locations where there are enough observations to calculate a monthly mean. References for the observations are in the text. The error bars represent different assumptions for calculated modeled A values for nighttime reactions as described in the text. Error bars for Beijing and Mt. Lulin reflect the range of possible modeled A values for nighttime reactions as described in the text. The  $y=x$  (solid line) and  $y = 2x$  and  $y = 0.5x$  (dashed) are shown.



1

2 **Figure S4.** Comparison of monthly-mean modeled and observed  $\Delta^{17}\text{O}(\text{nitrate})$ . Model points are from  
 3 the “cloud chemistry” simulation, while the modeled error bars reflect the full range of calculated values  
 4 from all sensitivity simulations. Error bars for the observations reflect the analytical uncertainty in the

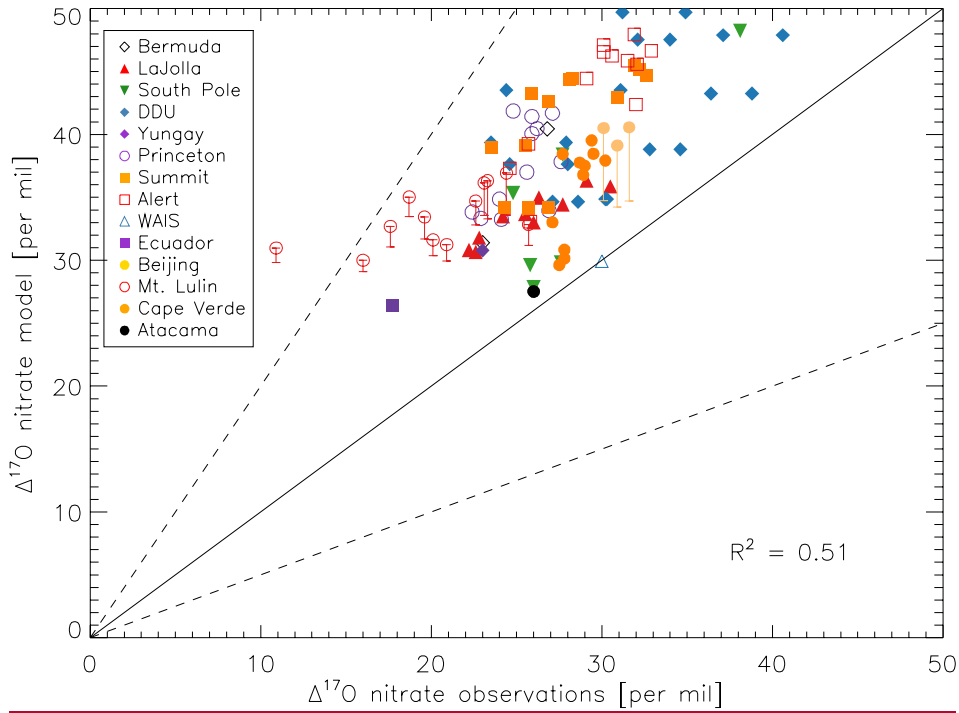
1 measurements, except for two data points in June for Summit which reflect the standard deviation of  
2  $\Delta^{17}\text{O}(\text{nitrate})$  from multiple measurements during that month.



3 3.0 12.2 21.5 30.8 40.0 [permil]

4 Figure S5. Modeled, annual-mean  $\Delta^{17}\text{O}(\text{NO}_2)$  below 1 km altitude for the "cloud chemistry" model.

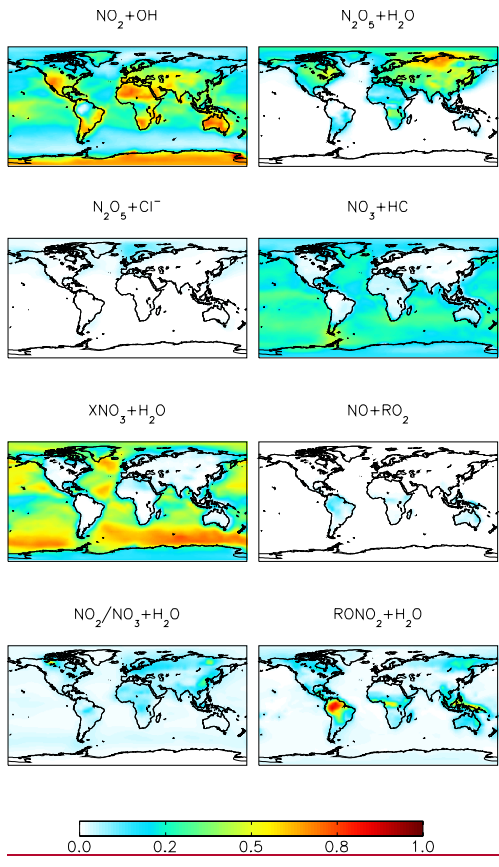
5  
6



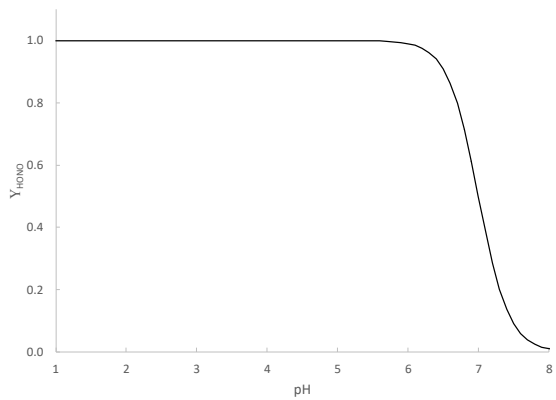
1

2 **Figure S6.** Same as Figure S3 but assuming  $\Delta^{17}\text{O}(\text{O}_3) = 35\text{‰}$ .

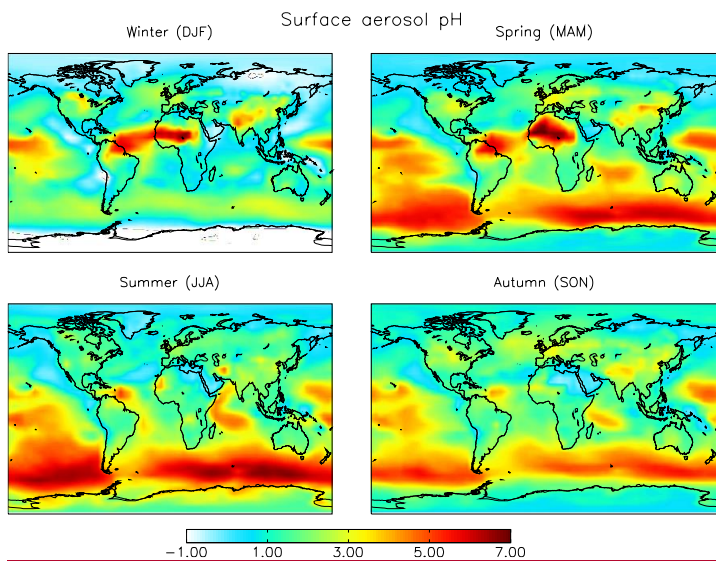
3



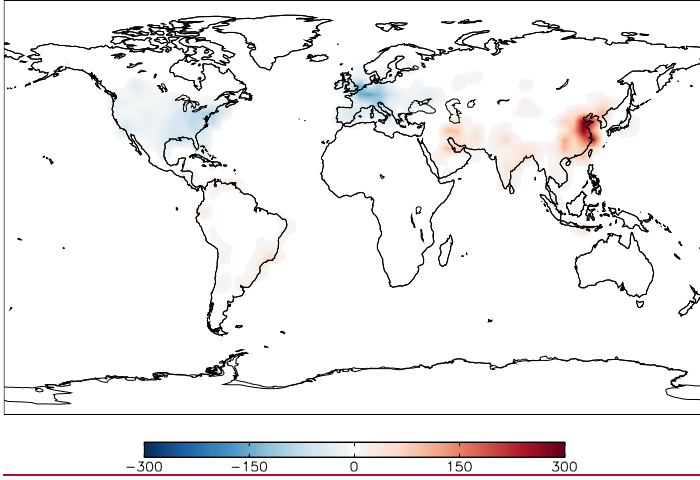
1  
2 **Figure S7.** Same as Figure 3 but for the “standard” simulation.  
3



1  
2  
3 **Figure S8.** Calculated yield of HONO from the heterogeneous reaction of  $\text{NO}_2$  on aerosol surfaces as a  
4 **function of pH.**



6  
7 **Figure S9.** Calculated surface aerosol pH in the model in each season.



1  
2  
3  
4  
5

**Figure S10.** Modeled change in anthropogenic NO emissions (Gg N yr<sup>-1</sup>) from the year 2000 to the year 2015 (2015 – 2000).